The Impact of Incomplete Nutrient Consumption in the Southern Ocean on Global Mean Ocean Nitrate $\delta^{15}N$

F. Fripiat[1,2] [ID], **D. M. Sigman[3]** [ID], **A. Martínez-García[2]** [ID], **D. Marconi[3]** [ID], **X. E. Ai[2,3]** [ID], **A. Auderset[2]** [ID], **S. E. Fawcett[4,5]** [ID], **S. Moretti[2]** [ID], **A. S. Studer[6]**, and **G. H. Haug[2]**

[1]Department of Geosciences, Environment and Society, Université Libre de Bruxelles, Brussels, Belgium, [2]Max Planck Institute for Chemistry, Mainz, Germany, [3]Department of Geosciences, Princeton University, Princeton, NJ, USA, [4]Department of Oceanography, University of Cape Town, Rondebosch, South Africa, [5]Marine and Antarctic Research Centre for Innovation and Sustainability (MARIS), University of Cape Town, Rondebosch, South Africa, [6]Department of Environmental Sciences, University of Basel, Basel, Switzerland

Abstract It is understood that the global mean ocean nitrate $\delta^{15}N$ is set by the $\delta^{15}N$ of the input of fixed nitrogen (N) to the ocean (mostly N_2 fixation) and the net isotopic discrimination of fixed N loss (mostly denitrification). Here, we demonstrate that, in addition to the fixed nitrogen input/output budget, the isotopic discrimination of nitrate assimilation in the Southern Ocean also plays a role in setting the $\delta^{15}N$ of both deep ocean nitrate and global mean ocean nitrate. A prognostic model is used to simulate the global overturning circulation, focusing on the Southern Ocean overturning cell that ventilates the global pycnocline. N_2 fixation and denitrification occur mainly in the model's surface and pycnocline boxes, as is appropriate given the observations. Experiments with this model indicate that, at a steady state, pycnocline nitrate $\delta^{15}N$ is mostly controlled by the ocean's fixed N budget. Simultaneously, partial nitrate assimilation in the Southern Ocean sets the nitrate $\delta^{15}N$ difference between the pycnocline and the deep ocean, lowering the $\delta^{15}N$ of deep ocean nitrate and thus also of global mean ocean nitrate. The Southern Ocean's impact on deep and mean ocean nitrate $\delta^{15}N$ depends on (a) the degree of nitrate consumption in the Southern Ocean surface waters and (b) the proportion of water that enters the pycnocline by subduction from the Southern Ocean surface. Including the effect of the Southern Ocean on mean ocean nitrate $\delta^{15}N$ modestly reduces a previously calculated imbalance between fixed N inputs and outputs. Moreover, this effect has implications for paleoceanographic N isotope records.

1. Introduction

Mean ocean nitrate $\delta^{15}N$ (i.e., $\delta^{15}N = \{^{15}N/^{14}N\}_{sample}/\{^{15}N/^{14}N\}_{reference} - 1$, with air N_2 as the reference) is thought to be set by the $\delta^{15}N$ of the fixed nitrogen (N) input and the net isotopic fractionation of fixed N removal (Brandes & Devol, 2002; Deutsch et al., 2004). Being the main source of fixed N to the ocean, N_2 fixation (and the subsequent nitrification of the newly fixed N) introduces nitrate to the ocean interior with a $\delta^{15}N$ of $\sim-1‰$ (Carpenter et al., 1997; cf. McRose et al., 2019; Minagawa & Wada, 1986). The removal of fixed N is mostly by water column and sedimentary denitrification (Bianchi et al., 2012; Brandes & Devol, 2002). In general, denitrification preferentially removes low-$\delta^{15}N$ nitrate and is thus instrumental in raising the $\delta^{15}N$ of ocean nitrate above that of N_2 fixation. Specifically, water column denitrification is associated with strong isotopic fractionation (Barford et al., 1999; Brandes et al., 1998; Casciotti et al., 2013; Cline & Kaplan, 1975; Kritee et al., 2012; Liu & Kaplan, 1989; Marconi, Kopf, et al., 2017), while the isotopic discrimination associated with sedimentary denitrification is typically much weaker (Brandes & Devol, 1997; Fripiat et al., 2018; Granger et al., 2011; Lehmann et al., 2004, 2007). Because of these differences in expressed isotope fractionation, the ratio of water column to sedimentary denitrification is a major control on nitrate $\delta^{15}N$, with a higher ratio yielding a higher nitrate $\delta^{15}N$ (Brandes & Devol, 2002; Deutsch et al., 2004).

If mean ocean nitrate $\delta^{15}N$ is representative of the fixed N budget, hereafter referred to as budget-driven nitrate $\delta^{15}N$ (i.e., N_2 fixation $\delta^{15}N$ + isotopic discrimination associated with denitrification), the isotopic distinction between water column and sedimentary denitrification provides an approach to estimate the relative importance of these fluxes in the removal of fixed N (Brandes & Devol, 2002; Deutsch et al., 2004; DeVries et al., 2013; Eugster & Gruber, 2012). This approach is especially useful given that water column denitrification is relatively well constrained in the literature (~70 Tg N yr^{-1}) in comparison to sedimentary denitrification (70–300 Tg N yr^{-1}) (Bianchi et al., 2012; Bohlen et al., 2012; Brandes & Devol, 2002; Codispoti et al., 2001; DeVries et al., 2012, 2013;
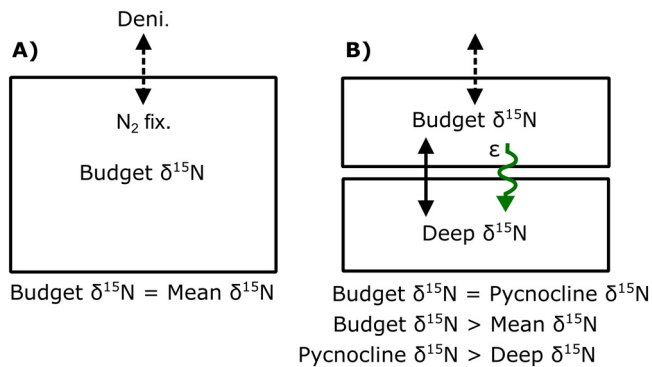
Figure 1. Schematic of a "one-box" ocean (a) and a two-box ocean (b). Dashed arrows indicate the addition and removal of nitrate by N_2 fixation (N_2 fix.) and denitrification (Deni.), solid black arrows represent water exchange terms, and the curved green arrow represents the export of organic N from the upper ocean that derived from partial nitrate assimilation in high latitude regions, which occurs with isotopic discrimination (ε). Panel (a) is representative of a homogenous (i.e., one-box) ocean in a steady state (Brandes & Devol, 2002). In this case, the mean ocean nitrate $\delta^{15}N$ ("mean $\delta^{15}N$") is set solely by the $\delta^{15}N$ of the input and the net isotopic fractionation of fixed N removal acting simultaneously in the same reservoir (the budget-driven nitrate $\delta^{15}N$; "budget $\delta^{15}N$"). In (b), all N_2 fixation and denitrification occurs in the pycnocline box, while there is an exchange of nitrate between the pycnocline and deep boxes. The preferential transfer of ^{14}N to the deep box by the sinking of low-$\delta^{15}N$ organic matter and its remineralization to nitrate implies that nitrate $\delta^{15}N$ in the deep box ("deep $\delta^{15}N$") is lower than the pycnocline box nitrate $\delta^{15}N$. The nitrate $\delta^{15}N$ of the pycnocline is forced to the budget-driven nitrate $\delta^{15}N$. The net effect is to decrease the deep ocean and thus mean ocean nitrate $\delta^{15}N$ relative to the budget-driven nitrate $\delta^{15}N$. Supplementary information text S1 provides the solution of the mass and isotopic balances.

Eugster & Gruber, 2012; Middelburg et al., 1996). The large uncertainty in the sedimentary denitrification rate yields a total denitrification rate that is either similar to or greater than the fixed N inputs to the ocean, implying either a balanced or unbalanced fixed N budget depending on whether the lower or upper range of sedimentary denitrification rate estimates is correct.

The isotope effect (ε) expresses the degree of isotopic discrimination and is defined in terms of the ratio of reaction rates at which the two isotopes are converted from reactant to product ($\varepsilon = \{1 - {}^{15}k/{}^{14}k\}$; where $^x k$ is the rate constant for the $^x N$-containing reactant). Early estimates of the isotope effect for water column denitrification ranged between 20 and 30‰ (Brandes et al., 1998; Voss et al., 2001). Assuming a homogenous ocean in the steady state, such a large isotope effect would require that water column denitrification accounts for only a small fraction of the fixed N loss from the ocean, implying sedimentary denitrification rates in the upper range of literature estimates (Brandes & Devol, 2002). Large isotope effects are supported in some culture experiments (Barford et al., 1999), but lower isotope effects (~13‰) have been reported from experiments with bacterial metabolic rates that more closely match natural conditions (Kritee et al., 2012). These lower estimates also match more recent field estimates that specifically examine the relationship between nitrate concentration and $\delta^{15}N$ along isopycnals (Casciotti et al., 2013; Ryabenko et al., 2012) and are also supported by some model/data comparisons (Marconi, Kopf, et al., 2017). In addition, the exchange of water between suboxic zones, where water column denitrification consumes a significant fraction of the nitrate pool, and waters outside suboxic zones biases the mixing product toward the end-member with the higher nitrate concentration. This process weakens the transmission of the elevated $\delta^{15}N$ signal into the global ocean and yields an under-expression of the organism-scale isotope effect at the scale of the environment (the "dilution effect"; Deutsch et al., 2004). Taking into consideration the dilution effect and/or using the lower range of estimates for the organism-scale

isotope effect of denitrification, a larger contribution of water column denitrification is required to generate the observed mean ocean nitrate $\delta^{15}N$. This implies, in turn, sedimentary denitrification rates at the lower end of literature estimates and, therefore, a fixed N budget for the global ocean that is closer to balanced (Deutsch et al., 2004; DeVries et al., 2013; Eugster & Gruber, 2012; Marconi, Kopf, et al., 2017; Somes et al., 2013).

An important caveat to the analysis above relates to the assumption that the global mean ocean nitrate $\delta^{15}N$ is representative of the fixed N budget. This assumption implies that N_2 fixation and denitrification occur in a homogenous (i.e., "one-box") ocean (Brandes & Devol, 2002), in which case the mean ocean nitrate $\delta^{15}N$ is set solely by the $\delta^{15}N$ of N_2 fixation and the net isotopic discrimination of denitrification (i.e., mean ocean nitrate $\delta^{15}N$ is equivalent to the "budget-driven nitrate $\delta^{15}N$"; Figure 1a). However, in an ocean where N_2 fixation and denitrification are spatially confined to one specific volume, it is the nitrate $\delta^{15}N$ of that volume that is set to the budget-driven nitrate $\delta^{15}N$ (Figure 1b). If there is no isotopic discrimination in the exchange of N between that volume and the rest of the ocean, then the mean ocean nitrate $\delta^{15}N$ will equal the budget-driven nitrate $\delta^{15}N$. However, this is not the case if, in the exchange of fixed N between the volume hosting the N budget terms and the rest of the ocean's volume, there are fluxes that occur with discrimination between the two N isotopes (e.g., partial nitrate assimilation followed by organic matter export and remineralization; Figure 1b). Rather, the rest of the ocean will harbor a nitrate $\delta^{15}N$ value that differs from the budget-driven nitrate $\delta^{15}N$ by a magnitude dictated by the isotopic discrimination of the N exchange processes (Figure 1; Text S1 in Supporting Information S1).

Observations and models indicate that both N_2 fixation and denitrification are spatially confined to the ocean's upper water column (i.e., roughly the upper 1.2 km, hereafter referred to as the pycnocline) (Bianchi et al., 2012; Deutsch et al., 2007; Wang et al., 2019). Moreover, partial nitrate assimilation in the Southern Ocean induces an isotope fractionation between the deep and upper ocean (i.e., preferentially incorporating ^{14}N into exported organic matter and leaving the residual surface nitrate pool enriched in ^{15}N) (Figure 2) (Sigman et al., 2009). These considerations imply that the pycnocline is set to the budget-driven nitrate $\delta^{15}N$, while the preferential
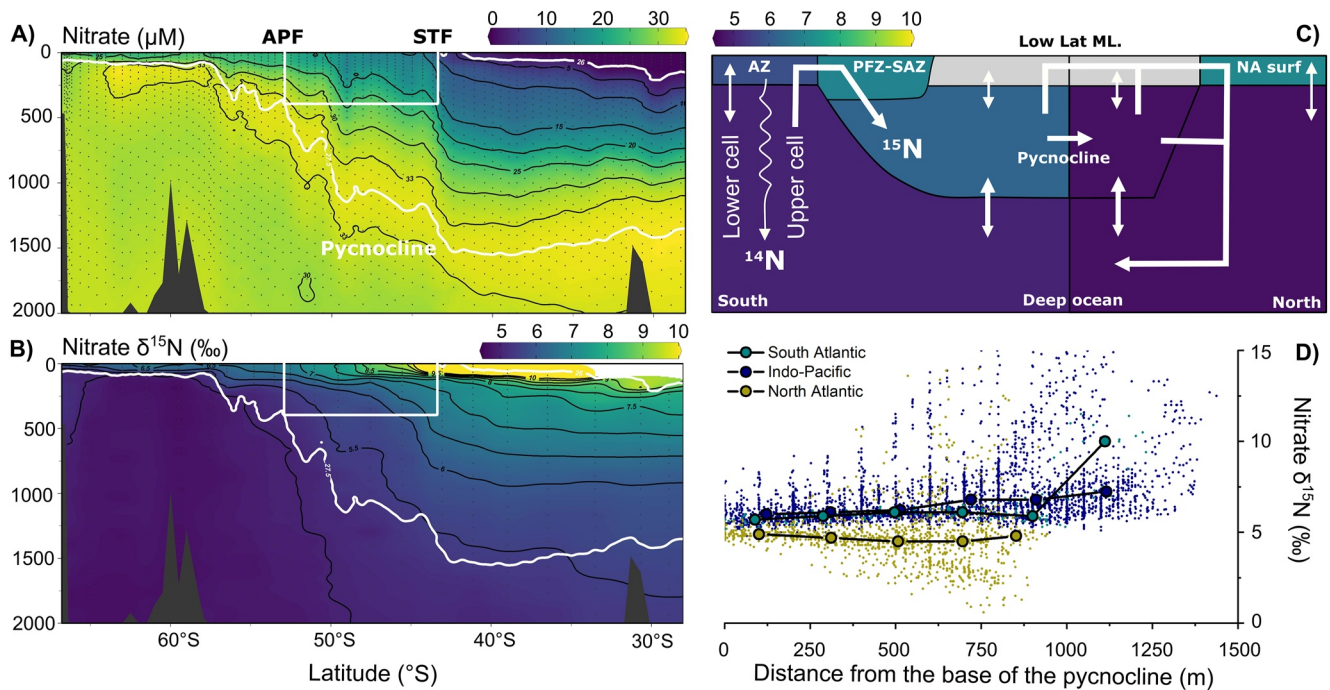
Figure 2. Meridional depth sections of nitrate concentration (a) and nitrate $\delta^{15}N$ (b) in the Indian sector of the Southern Ocean at 78–95°E (IO8S GOSHIP section) (adapted from Fripiat, Martínez-García, et al., 2021). The 26.0 and 27.5 g kg^{-1} isopycnals are shown with thick white lines. The white rectangle outlines the average winter mixed layer in the PFZ-SAZ (Dong et al., 2008). These boundaries define several of the reservoirs in the prognostic ocean models (c), with the colors representing the weighted nitrate $\delta^{15}N$ computed in Fripiat, Martínez-García, et al. (2021) from a large-scale nitrate $\delta^{15}N$ database (Fripiat, Marconi, et al., 2021). (d) Nitrate $\delta^{15}N$ versus the distance from (i.e., above) the base of the pycnocline in the South Atlantic (petrol), the North Atlantic (olive), and the Indo-Pacific basin (dark-blue). The median-profiles for each basin are shown with the larger symbols. Strongly elevated nitrate $\delta^{15}N$ near the surface in the South Atlantic (reflected in the particularly high $\delta^{15}N$ of the shallowest binned depth interval) is caused by the isotopic discrimination of partial nitrate assimilation just north of the Subtropical Front, where the pycnocline is the deepest (i.e., 34.5°S). Abbreviations are as follows: AZ, Antarctic Zone; PFZ, Polar Front Zone; SAZ, Subantarctic Zone; APF, Antarctic Polar Front; STF, Subtropical Front; Low Lat. ML, low latitude-mixed layer; NA surf, North Atlantic surface water.

accumulation of ^{14}N in the deep ocean lowers its $\delta^{15}N$ value relative to the budget-driven nitrate $\delta^{15}N$. To validate this inference and explore its implications, we further developed and applied a simple prognostic, isotope-enabled model of the ocean's N cycle (Figure 3; Fripiat, Martínez-García, et al., 2021). With it, we tested various treatments of N$_2$ fixation and denitrification. We also explore the impact of the meridional overturning circulation, specifically varying the degree to which deep ocean water returns to the pycnocline by Southern Ocean wind-driven upwelling *vs.* mixing-driven upwelling in the ocean interior. Finally, the impact of the degree to which nitrate is consumed in Southern Ocean surface waters is considered. From the model results, we quantify and characterize the Southern Ocean's impact on deep ocean and mean ocean nitrate $\delta^{15}N$ and discuss the implications for (a) the ratio of water column to sedimentary denitrification, (b) the degree of nitrate consumption in the Southern Ocean during ice ages, and (c) deglacial changes in the ocean's fixed N budget.

2. Prognostic Ocean Model of Nitrate Isotopes

2.1. Five-Box Model

A prognostic five-box ocean model was constructed by Fripiat, Martínez-García, et al. (2021) to confirm assumptions associated with a one-box model (i.e., to consider the effect of the fixed N budget). In that study, the one-box model and a large-scale nitrate isotope data compilation (Fripiat, Marconi, et al., 2021) were used to place observational constraints on the sources of nutrients to the global pycnocline. Here, we further develop and apply the prognostic multi-box ocean model to constrain the systematics of N isotopes at the global scale.

In this model version, the ocean is divided into five boxes: the deep ocean, the pycnocline, the Antarctic Zone (AZ) surface water, the Polar Frontal Zone and Subantarctic Zone (PFZ-SAZ) ventilating area and the low-latitude surface water (Figure 3a). The lower boundary of the pycnocline is defined by the 27.5 g kg^{-1} isopycnal, sitting at
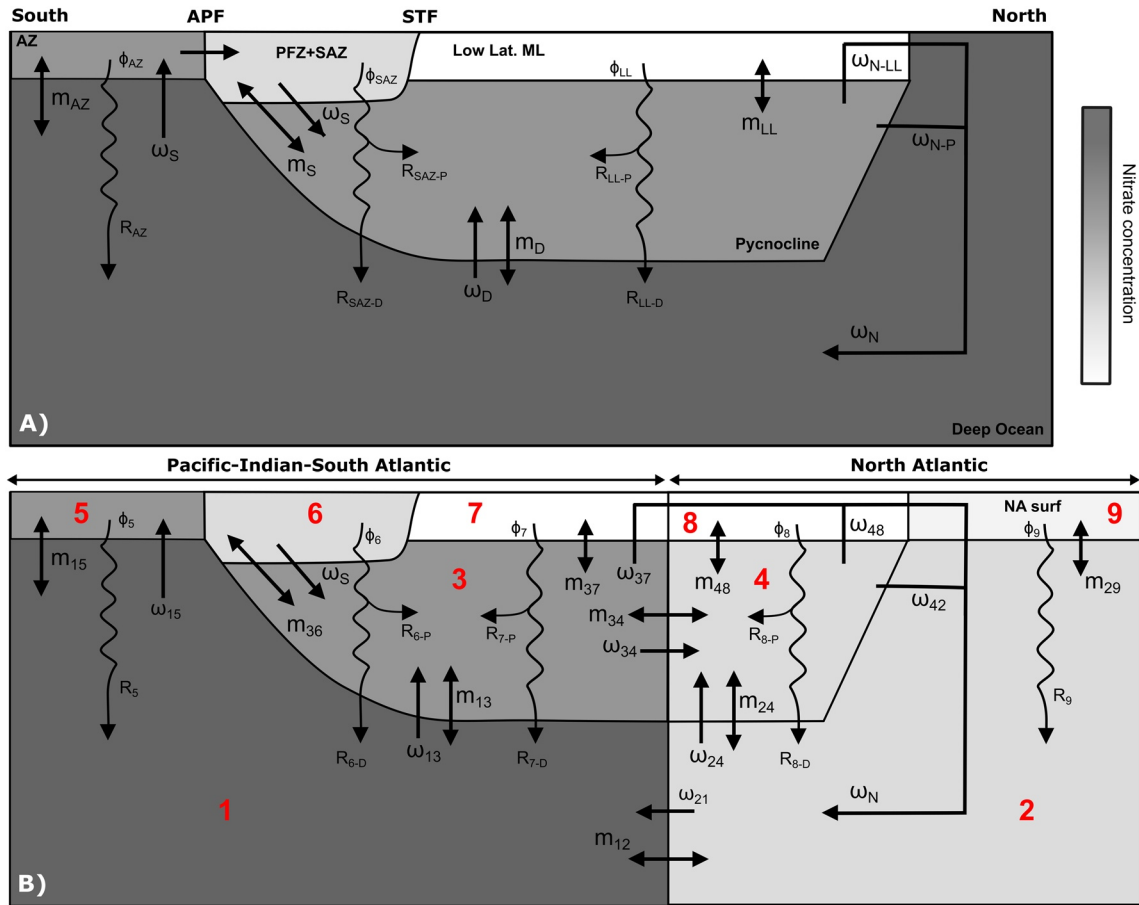
Figure 3. Schematics of the reservoirs and processes included in the prognostic five-box ocean model (a; adapted from Fripiat, Martínez-García, et al., 2021) and in the prognostic nine-box ocean model (b). Straight arrows represent water exchange fluxes either by large-scale advection (ω terms) or mixing (m terms), while wavy arrows indicate export production and remineralization. These terms are described in Table 1. The addition and removal of nitrate by N_2 fixation and denitrification are not shown and are confined to the pycnocline and the overlying surface (see Section 3.1.2). In Text S2 in Supporting Information S1, a model version is described that includes a portion of N_2 fixation and sedimentary denitrification occurring in the deep ocean. Abbreviations are as follows: AZ, Antarctic Zone; PFZ, Polar Front Zone; SAZ, Subantarctic Zone; APF, Antarctic Polar Front; STF, Subtropical Front; Low Lat. ML, low latitude-mixed layer; NA surf, North Atlantic surface water.

~1,000–1,500 m depth in the low-latitude ocean and outcropping near the Antarctic Polar Front in the Southern Ocean and near the Subarctic Front in the North Atlantic. This boundary corresponds to the base of Antarctic Intermediate Water, which is apparent as the mid-depth salinity minimum spreading northward in the different ocean basins. In the North Pacific and Indian basins, this isopycnal does not outcrop in the North; the northern limit in these basins is the continental shelves. Between the Antarctic Polar Front and the Subtropical Front, the upper pycnocline boundary is the winter mixed layer depth (~400 m depth; Dong et al., 2008). Above this boundary and up to the surface is the region we define as the combined PFZ-SAZ ventilating area. North of the Subtropical Front, the upper pycnocline boundary is the depth of the 26.0 g kg^{-1} isopycnal. Above this boundary and up to the surface is defined here as the low-latitude surface mixed layer, in which nutrients are nearly completely consumed. South of the Antarctic Polar Front and above the winter mixed layer depth (~150 m depth; Dong et al., 2008) is the region we define as the AZ surface water layer.

Water and dissolved constituents are exchanged among the different domains either by large-scale advective fluxes (ω terms) or mixing fluxes (m terms) (Figure 3a). The large-scale advective fluxes include the "upper cell" of the meridional overturning circulation (ω_S), where the southern hemisphere westerly winds drive upwelling in the AZ and northward transport toward the combined PFZ-SAZ ventilating area (Marshall & Speer, 2012). There, Antarctic Intermediate Water and Subantarctic Mode Water are subducted into the pycnocline at the Antarctic Convergence (again, ω_S). Upwelling in the interior from the deep ocean to the pycnocline (ω_D) is induced by small-scale turbulent mixing that transports heat downward and thus increases the buoyancy of deep waters

Table 1
Model Parameters (Figure 3a) and Ranges for the Different Model Experiments

Scenario	Optimized[a],*	Sensitivity test[b],*	Time-dependent**
m_{AZ} (Sv)—Southern Ocean lower overturning cell, diapycnal, and isopycnal mixing	20	20	20
ω_S (Sv)—Southern Ocean upper overturning cell (i.e., residual)	0–37 or 33	0–100 or 33	33.3 or 3.7–33.3
m_S (Sv)—Isopycnal mixing (i.e., eddy diffusion)	$1.5 \cdot \omega_S$	0–100 or $1.5 \cdot \omega_S$	$1.5 \cdot \omega_S$
ω_D (Sv)—Interior upwelling rate	0–37 or 4	0–100 or 4	3.7 or 3.7–33.3
m_D (Sv)—Diapycnal mixing in the ocean interior	$6.0 \cdot \omega_D$	0–100 or $6.0 \cdot \omega_D$	$6.0 \cdot \omega_D$
$\omega_{N\text{-}LL}/(\omega_{N\text{-}LL} + \omega_{N\text{-}P})$ (five-box model) or $\omega_{37}/(\omega_{37} + \omega_{34})$ (nine-box model)	0.82	0.5–1.0	0.82
$\omega_{48}/(\omega_{48} + \omega_{42})$ (nine-box model)	0.05	0.0–0.1	0.05
m_{12} (Sv)—Mixing flux in the deep ocean (nine-box model)	25	0–50	25
m_{34} (Sv)—Mixing flux in the pycnocline (nine-box model)	5	0–50	5
m_{29} (Sv)—Mixing flux with the North Atlantic surface (nine-box model)	20	20	20
m_{LL} (Sv)—Mixing with the low-latitude mixed layer	18.7	0–50	18.7
$f_{\phi\text{-}LL}$—Fraction of low-lat. nutrient supply being exported with ϕ_{LL}	1.00	1.00	1.00
$f_{R\text{-}LL}$ (in the pycnocline)[c]—Fraction of ϕ_{LL} being remineralized in the pycnocline	0.85	0.8–0.9	0.85
$f_{\phi\text{-}AZ}$—Fraction of AZ nutrient supply being exported with ϕ_{AZ}	0.23 or 0.0 to 1.0	0.23 or 0.0 to 1.0	0.23–0.95
$f_{R\text{-}AZ}$—Fraction of ϕ_{AZ} being remineralized in the deep ocean	1.0	1.0	1.0
$f_{\phi\text{-}SAZ}$—Fraction of SAZ nutrient supply being exported with ϕ_{SAZ}	0.35 or 0.0 to 1.0	0.35 or 0.0 to 1.0	0.35–0.95
$f_{R\text{-}SAZ}$ (in the pycnocline)[c]—Fraction of ϕ_{SAZ} being remineralized in the pycnocline	0.23	0.0–0.5	0.23
$f_{\phi\text{-}9}$—Fraction of North-Atl. nutrient supply being exported with ϕ_9 (nine-box model)	0.6	0.5–0.8	0.6
$f_{R\text{-}9}$—Fraction of ϕ_9 being remineralized in the deep ocean (nine-box model)	1.0	1.0	1.0
Denitrification (Tg N yr^{-1})	150	100–250	150
% of total denitrification in the pycnocline[d]	85–100	85–100	100
ε_{ass}[e] (‰)—Isotope effect for nitrate assimilation	5.5	5.5	5.5
ε_{deni} (‰) in the pycnocline—Net isotope effect for denitrification	7.25–8.30	7.25–8.30	7.25
ε_{deni} (‰) in the Indo-Pacific and South-Atlantic pycnocline	8.00	8.00–9.20	8.00
ε_{deni} (‰) in the deep ocean or in the North Atlantic pycnocline	0	0	0
N$_2$ fixation δ^{15}N (‰)	−1	−1	−1

[a]Values for some of the model parameters constrained in Fripiat, Martínez-García, et al. (2021). [b]Randomly varying model parameters ($n = 100{,}000$) over this sensitivity range for each model scenario. [c]The remaining fraction is remineralized in the deep ocean. [d]The remaining fraction is occurring in the deep ocean. [e]The isotope effect in the PFZ-SAZ ventilating area is divided by 4 given the ratio of surface water to winter-mixed layer depth. *In the model scenario with either a varying overturning ratio (left values; Fig. 5a, 5c, 5e) or varying degree of nitrate consumption in the PFZ–SAZ and AZ (right values; Fig. 5b, 5d, 5f) represented by the trajectories in Fig. 4 **In the model scenario with either a constant overturning ratio (left values; Fig. 8a, 8b) or with a varying overturning ratio (right values; Fig. 8c, 8d, 8e, 8f)

(Bryan, 1987; Talley, 2013). In the pycnocline, these large-scale advective fluxes ($\omega_S + \omega_D$) flow northward to contribute to the formation of North Atlantic Deep Water (ω_N), which is partitioned between surface ($\omega_{N\text{-}LL}$) and intermediate ($\omega_{N\text{-}P}$) flows. The surface exposure of the "lower cell" is entirely within the AZ (Lumpkin & Speer, 2007) and is represented in the model by a mixing term (m_{AZ}), which also includes any other exchange terms such as diapycnal and isopycnal mixing as well as deep water formation. Other mixing terms include isopycnal mixing between the PFZ-SAZ ventilating area and the pycnocline (m_S), diapycnal mixing between the deep ocean and the pycnocline (m_D), and mixing between the pycnocline and low-latitude surface water (m_{LL}).

Export production (ϕ) is controlled by the gross nitrate supply into the surface layer (i.e., water fluxes times nitrate concentration in the source water) and the degree of nitrate consumption (f_ϕ = nitrate uptake/gross nitrate supply). Export production is regenerated (R) either within the pycnocline (that fraction being termed f_R, i.e., = remineralization/export production) or in the underlying deep ocean; in the AZ, all export is remineralized in the deep ocean. Nitrate assimilation is assumed to proceed with a kinetic isotope effect (ε_{ass}) of 5.5‰ (Fripiat et al., 2019; Sigman et al., 1999). The δ^{15}N of export production ($\phi\,\delta^{15}$N) is described by Rayleigh fractionation kinetics (accumulated product), making it a function of f_ϕ and ε_{ass} (Fripiat et al., 2019). Complete consumption of
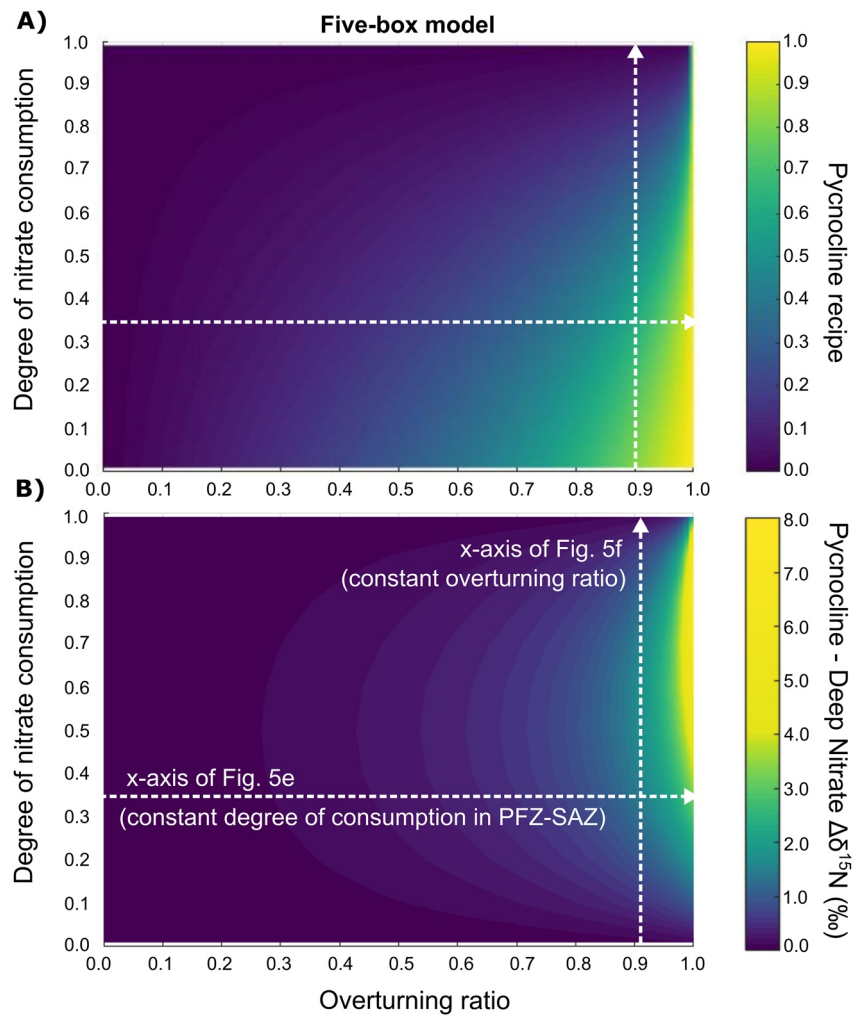
Figure 4. In the five-box model, the effects of the degree of Southern Ocean nitrate consumption and the ratio of $\omega_S/(\omega_S + \omega_D)$ (i.e., the overturning ratio) on the pycnocline recipe (a; Equation 3) and the difference in nitrate $\delta^{15}N$ ($\Delta\delta^{15}N$) between the pycnocline and the deep ocean (b). The mixing terms (m_S and m_D) are held in a constant proportion to the advective terms (ω_S and ω_D, respectively). At any location in the plotted parameter space, the other model parameters are held constant at those values that resulted from the optimization of the model to best-fit nitrate isotope data and other measurements (Fripiat, Martínez-García, et al., 2021) (i.e., optimized model experiment in Table 1). The optimized model experiment trajectories (white dashed arrows) consist of either varying the overturning ratio (horizontal arrows; x-axis in Figures 5a, 5c, 5e, 7a and 7c) or the degree of nitrate consumption in both AZ and PFZ-SAZ (vertical arrows; x-axis in Figures 5b, 5d, 5f, 7b and 7d).

nitrate ($f_\phi = 1$) implies no expression of isotopic discrimination by nitrate assimilation and an export production $\delta^{15}N$ that is equal to the $\delta^{15}N$ of the nitrate supply (Altabet & François, 1994). The $\delta^{15}N$ of the nitrate added to the ocean interior by remineralization is determined by the $\delta^{15}N$ of the N exported from the surface ocean (i.e., R $\delta^{15}N = \phi \, \delta^{15}N$) (Marconi et al., 2019; Rafter et al., 2013).

In the default version of the five-box model, N$_2$ fixation (N$_2$-fix) is prescribed to be occurring entirely in the low latitude surface, ultimately to be remineralized to nitrate in the pycnocline. In addition, denitrification (Deni) is prescribed to be taking place in the pycnocline or overlying surface. These appear to be reasonable approximations of the real ocean. First, N$_2$ fixation occurs mostly in the low-latitude mixed layer, producing new nitrate largely through low-latitude export production of organic N and its remineralization in the shallow ocean interior (Gruber & Sarmiento, 1997). Moreover, most of the water column denitrification occurs in the suboxic zones of the pycnocline (Deutsch et al., 2001), and the bulk of sedimentary denitrification occurs on the seafloor at depths within the pycnocline or the overlying surface mixed layer (Bianchi et al., 2012). In Text S2 in Supporting Information S1, a model version is described that includes the remineralization of a portion of the sinking organic

matter deriving from N$_2$ fixation in the deep ocean as well as a portion of the sedimentary denitrification occurring in the deep ocean. Finally, a balance between N$_2$ fixation and denitrification is assumed.

In this model, N$_2$ fixation introduces nitrate with a prescribed δ^{15}N value of −1‰ (Carpenter et al., 1997; Minagawa & Wada, 1986). Denitrification removes nitrate with a net isotope effect ($\varepsilon_{\text{deni}}$) that combines the isotope effect for sedimentary and water column denitrification. In this approximation of a balanced budget (i.e., denitrification rate = N$_2$ fixation rate), we are not considering smaller components of the budget, which include terrestrial river input and atmospheric deposition (Altieri et al., 2021; Brandes & Devol, 2002).

The model is run for 20,000 model years, allowing a whole-ocean N$_2$ fixation – denitrification balance to be reached. Below, we show conservation equations for ^{14}N (Equation 1) and ^{15}N (Equation 2) for a hypothetical subsurface box i exchanging water with a hypothetical surface box j, supplying nutrients to box j, which feeds export production from box j to box i, followed by remineralization in box i:

$$V_i \cdot \frac{d^{14}N_i}{dt} = \omega_{ij} \cdot {}^{14}N_j - \omega_{ji} \cdot {}^{14}N_i + m_{ij} \cdot \left({}^{14}N_j - {}^{14}N_i \right) + f_\varnothing \cdot f_R \cdot (m_{ij} + \omega_{ij}) \cdot {}^{14}N_i + N_{2-\text{fix}} - \text{Deni} \quad (1)$$

$$V_i \cdot \frac{d^{15}N_i}{dt} = \omega_{ij} \cdot {}^{15}N_j - \omega_{ji} \cdot {}^{15}N_i + m_{ij} \cdot \left({}^{15}N_j - {}^{15}N_i \right) + f_\varnothing \cdot f_R \cdot (m_{ij} + \omega_{ij}) \cdot {}^{15}N_i \cdot \left(\frac{1 - (1 - f_\varnothing)^{1 - \frac{\varepsilon_{ass}}{1000}}}{f_\varnothing} \right)$$

$$+ N_{2-fix} \cdot {}^{15}R_{N2-\text{fix}} - \text{Deni} \cdot {}^{15}R_i \cdot \left(1 - \frac{\varepsilon_{\text{deni}}}{1000} \right) \quad (2)$$

where V_i is the volume (l) of box i, $^{14}N_i$ is the concentration of ^{14}N-nitrate (μmol l^{-1}), $^{15}N_i$ for ^{15}N-nitrate (μmol l^{-1}), ω_{ij} is the large-scale advective flux (l yr^{-1}) from box j to i, ω_{ji} is the large scale advective flux from box i to j, m_{ij} is the mixing flux (l yr^{-1}) between box i and j, N$_{2\text{-fix}}$ is the N$_2$ fixation flux for ^{14}N (μmol yr^{-1}), Deni is the denitrifictaion flux for ^{14}N (μmol yr^{-1}), $^{15}R_i$ is the ^{15}N/^{14}N ratio of nitrate in box i, and $^{15}R_{N2-fix}$ is the ^{15}N/^{14}N ratio of N$_2$ fixation.

2.2. Nine-Box Model

In the prognostic five-box model, the pycnocline is treated as a homogeneous reservoir (i.e., as one box). In the real ocean, isotopic gradients are observed across the pycnocline, with the strongest gradients at the boundaries of the Oxygen Minimum Zones (OMZs) and the North Atlantic Ocean. Outside these areas, relatively constant depth-weighted δ^{15}N values are reported with small isotopic gradients (<0.2‰) across ocean basins (Figure 2d; Table S1 in Supporting Information S1) (Fripiat, Marconi, et al., 2021; Fripiat, Martínez-García, et al., 2021). In the North Atlantic, low depth-weighted δ^{15}N values are observed (Figure 2d), which have been attributed to an excess of N$_2$ fixation relative to denitrification and a lack of water column denitrification (Deman et al., 2021; Fawcett et al., 2015; Knapp et al., 2005, 2008; Marconi et al., 2015; Marconi, Sigman, et al., 2017). In the OMZs, water column denitrification raises the residual nitrate δ^{15}N above the mean pycnocline value (Casciotti et al., 2013; Liu & Kaplan, 1989; Martin & Casciotti, 2017; Sigman et al., 2005). The North Atlantic-influenced area represents 6.5% of the nitrate pool in the pycnocline, the OMZ-influenced area 17.1%, and the remaining low-latitude area 76.4%. The nitrate of the North Atlantic lowers pycnocline-wide nitrate δ^{15}N by 0.10‰, while the OMZs raise pycnocline-wide nitrate δ^{15}N by 0.28‰. The two regions, taken together, increase the mean pycnocline nitrate δ^{15}N by 0.21‰ (i.e., from 6.04 to 6.25‰) (Fripiat, Martínez-García, et al., 2021).

Interbasin gradients can introduce systematic error if there is a spatial correlation between cross-pycnocline transport and the nitrate concentration and δ^{15}N gradients between the pycnocline and the underlying deep ocean. The most important case of this is the North Atlantic, where North Atlantic Deep Water (NADW) sinks into the ocean interior (ω_N). The low nitrate δ^{15}N values reported in this basin may contribute to the low-δ^{15}N values in the deep ocean. To consider this effect, we developed a prognostic nine-box ocean model (Figures 2c and 3b), where the global pycnocline and the deep ocean are each divided into two boxes (i.e., the North Atlantic basin and the combined Indo-Pacific and South Atlantic basins). We add a surface box in the North Atlantic to represent the subpolar gyre and the NADW sinking region. As explained above, this model configuration is supported by the observations where relatively similar depth-weighted δ^{15}N values are reported in the Indo-Pacific and South Atlantic pycnoclines (Table S1 in Supporting Information S1; Figure 2d).

In this configuration, the large-scale advective and mixing fluxes from the deep ocean (ω_D and m_D) are partitioned between the combined Indo-Pacific and South Atlantic basins (ω_{13} and m_{13}) and the North Atlantic basin (ω_{24} and m_{24}), according to the relative contribution of their area to the global pycnocline (i.e., 0.88 and 0.12, respectively) (Figure 3b). We follow the same rationale for the mixing fluxes between the pycnocline and the low-latitude mixed layer (m_{LL}), that is, m_{37} and m_{48}, respectively. ω_D is, therefore, the sum of ω_{13} and ω_{24}, m_D the sum of m_{13} and m_{24}, and m_{LL} the sum of m_{37} and m_{48}. In the pycnocline, large-scale advective fluxes flow from the combined Indo-Pacific and South Atlantic basins to the North Atlantic basin, and are partitioned between surface (ω_{37}) and intermediate (ω_{34}) fluxes. These advective fluxes combine with ω_{24} in the North Atlantic basin to contribute to the formation of the North Atlantic Deep Water (ω_N), which is partitioned between surface ($\omega_{N-LL} = \omega_{37} + \omega_{48}$) and intermediate ($\omega_{N-P} = \omega_{42}$) outflows. There are lateral mixing fluxes between the combined Indo-Pacific and South Atlantic pycnocline and the North Atlantic pycnocline (m_{34}), as well as in the deep ocean (m_{12}). The "lower cell" is still represented in the model by a mixing term ($m_{15} = m_{AZ}$), and we also include a mixing term between the North Atlantic surface box with the deep ocean (m_{29}).

In order to match the nitrate concentration observed in the North Atlantic pycnocline, the routing of the advective flow through the surface (ω_{48} *vs.* ω_{42}) must be severely reduced in comparison to the combined Indo-Pacific and South Atlantic pycnocline (ω_{37} *vs.* ω_{34}) (Table 1). Complete nutrient consumption in low-latitude surface waters requires that the nutrients supplied to these waters by the advective flow are mostly returned to the pycnocline via export production and remineralization (i.e., effectively "trapping" nutrients in the pycnocline). Keeping the same partitioning between surface and intermediate outflows in the North Atlantic pycnocline as in the combined Indo-Pacific and South Atlantic pycnocline would impliy a similar advective flow through the surface, yielding a similar export of nutrients (in µmol yr^{-1}) and remineralization into the pycnocline, but redistributed to a much smaller volume. This would yield nutrient concentrations in the North Atlantic pycnocline that are far higher than observed.

For export production (ϕ) and remineralization (R), we follow the same rationale as in the five-box model. To implement the observed excess of N$_2$ fixation in comparison to denitrification in the North-Atlantic while maintaining a balance between N$_2$ fixation and denitrification at the scale of the global pycnocline, we run the model assuming that 17% and 10% of N$_2$ fixation and denitrification (i.e., all as sedimentary denitrification) occurs in the North Atlantic pycnocline, respectively, yielding a 7% excess in N input (Bianchi et al., 2012; Deutsch et al., 2007; Marconi, Sigman, et al., 2017; Wang et al., 2019). This yields an excess of fixed N of 7–18 Tg N yr^{-1} in the North Atlantic basin (for a global N$_2$ fixation rate of 100–250 Tg N yr^{-1}, respectively), which is balanced by a deficit of the same amplitude in the combined Indo-Pacific and South Atlantic basins.

2.3. Model Experiments

We define two important parameters used to measure the degree to which deep waters (and associated nutrients) return to the upper ocean by upwelling in the Southern Ocean, as opposed to directly from the deep ocean by interior upwelling. As in Fripiat, Martinez-Garcia, et al. (2021), we use the term "pycnocline recipe":

$$\text{Pycnocline recipe} = (\Omega_S + M_S)/(\Omega_S + M_S + \Omega_D + M_D) \qquad (3)$$

with the capital letters Ω and M referring to the nitrate transport rates (in µmol N yr^{-1}) into the pycnocline by the large-scale advective water transport, ω, and by mixing, m. For example, Ω_S is the product of ω_S (in l yr^{-1}) and nitrate concentration (in µmol N l^{-1}) in the combined PFZ-SAZ ventilating area. We also consider an advection-only, water-only analogue, which we term the "overturning ratio":

$$\text{Overturning ratio} = \omega_S/(\omega_S + \omega_D) \qquad (4)$$

The pycnocline recipe is a function of (a) the proportion of water that enters the pycnocline from the Southern Ocean surface (i.e., the overturning ratio and mixing terms, m_S and m_D) and (b) the degree of nitrate consumption in southern surface waters (Figure 4a). We run the models by varying either of these two parameters in three configurations:

1. Optimized model experiments: Either the overturning ratio or the degree of nitrate consumption in both the AZ and PFZ-SAZ are varied (from 0 to 1; Figure 4), keeping the values of the other model parameters constant (Table 1). Except for m_{AZ}, m_{29}, m_{12}, and m_{34}, the values for the model parameters are those that resulted from

optimization of the model to best-fit nitrate isotope data and other measurements (Fripiat, Martínez-García, et al., 2021). For the exchanges of water between the PFZ-SAZ ventilating area and the pycnocline (m_S) and between the deep ocean and the pycnocline (m_D), mixing terms are varied to maintain a constant ratio with the corresponding advective terms (ω_S and ω_D, respectively). This assumption of a constant ratio is consistent with the general understanding of the relationships of isopycnal and diapycnal mixing with advection (Munk & Wunsch, 1998; Morrison & Hogg, 2012).

2. Sensitivity experiments: To test the sensitivity of the model to various important parameters, we vary those parameters over a range well beyond literature estimates (Table 1), holding m_{AZ} and m_{29} constant. For each model parameter, 100,000 random numbers are generated in the parameter sensitivity range, yielding the same number of model scenarios. Model runs with m_{AZ} and m_{29} varying from 0 to 100 Sv yield indistinguishable results from model runs keeping m_{AZ} and m_{29} constant (at 20 Sv each) (data not shown).

3. Transient simulations: To explore the temporal response of the system to a perturbation, such as would apply across a deglaciation, we run time-dependent simulations in which we change (a) the degree of nitrate consumption in the AZ surface water and PFZ-SAZ ventilating area ($f_{\phi-AZ}$ and $f_{\phi-SAZ}$), (b) the overturning ratio, or (c) both (Table 1). For the exchanges of water between the PFZ-SAZ ventilating area and the pycnocline (m_S) and between the deep ocean and the pycnocline (m_D), as for the optimized model experiments, each mixing term is varied so as to maintain a constant ratio with the corresponding advective term (ω_S and ω_D, respectively).

For the model experiments with varying degrees of nitrate consumption in Southern Ocean surface waters, we change the degree of nitrate consumption in the AZ and PFZ-SAZ equally. In the model experiments with varying proportions of water entering the pycnocline from the Southern Ocean surface, the degree of nitrate consumption in both the AZ and PFZ-SAZ is set to modern conditions (i.e., 0.23 and 0.35, respectively; Garcia et al., 2013).

3. Results and Discussion

3.1. Southern Ocean Impact on Mean Ocean Nitrate $\delta^{15}N$

3.1.1. Partial Nitrate Assimilation in the Southern Ocean

In the Antarctic Zone, nitrate is supplied from the deep ocean by Ekman upwelling and vertical mixing across the base of the winter mixed layer (Figure 2). Partial nitrate consumption by phytoplankton in the surface waters of the Southern Ocean raises the $\delta^{15}N$ of nitrate because of the preferential incorporation of ^{14}N into new biomass (Sigman et al., 1999). The surface footprint of the lower overturning cell occurs entirely in the AZ and includes some combination of vertical mixing and convection in the open AZ and deep water formation in the coastal AZ. Considering the nitrate supply, nitrate consumption, and sinking organic matter production associated with the lower cell, the remineralization of the sinking organic matter occurs entirely in the deep ocean. In this case, the ^{15}N enrichment in the subducted nitrate is counteracted by the remineralization of the resulting low-$\delta^{15}N$ product in the same water parcel. Thus, considering the lower overturning cell in isolation, the $\delta^{15}N$ of the combination of surface nitrate and sinking organic N transported from the AZ surface to the deep ocean will be equivalent to the $\delta^{15}N$ of the nitrate originally supplied from the deep ocean into the AZ surface. However, the upper overturning cell breaks this isotopic equivalence. In the upper cell, surface waters are transported northward by Ekman transport from the AZ to the PFZ and SAZ before entering the ocean interior as intermediate and mode waters. This circulation transports nitrate with an elevated $\delta^{15}N$ northward and into the pycnocline. Conversely, the regeneration of the low-$\delta^{15}N$ organic matter sinking from the Southern Ocean surface causes a lowering of the $\delta^{15}N$ of the deep ocean nitrate (Sigman et al., 2000).

The ocean's "internal nitrate cycle" includes nitrate supply to the surface by circulation and mixing, nitrate assimilation by phytoplankton, sinking of the resulting organic N into the ocean interior, and organic matter remineralization and nitrification returning nitrate to the interior waters. From the perspective of the internal nitrate cycle alone, the northward transport of elevated nitrate $\delta^{15}N$ by the Southern Ocean's upper cell raises the $\delta^{15}N$ of nitrate in the global pycnocline and lowers the $\delta^{15}N$ of nitrate in the deep ocean (Figure 5c) (Rafter et al., 2013; Sigman et al., 2009). In the low-latitude ocean, nitrate is consumed to completion, and so the $\delta^{15}N$ of sinking organic matter (and of the nitrate regenerated therefrom) is equal to the $\delta^{15}N$ of supplied nitrate on an annual basis (Altabet, 1988; Altabet & Francois, 1994). Accordingly, low-latitude nitrate supply, export production, and remineralization preserve the high-$\delta^{15}N$ imprint from the Southern Ocean on pycnocline nitrate
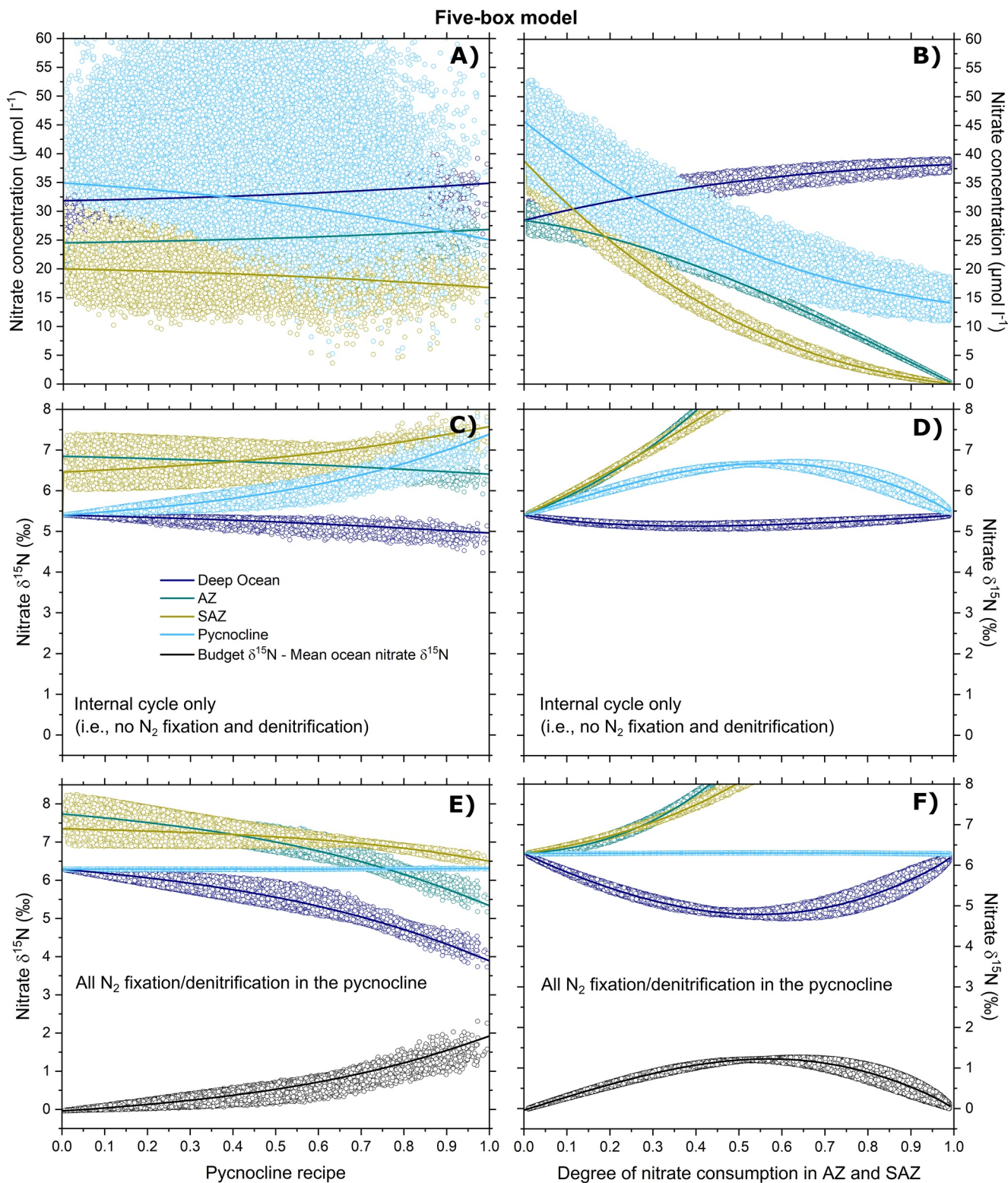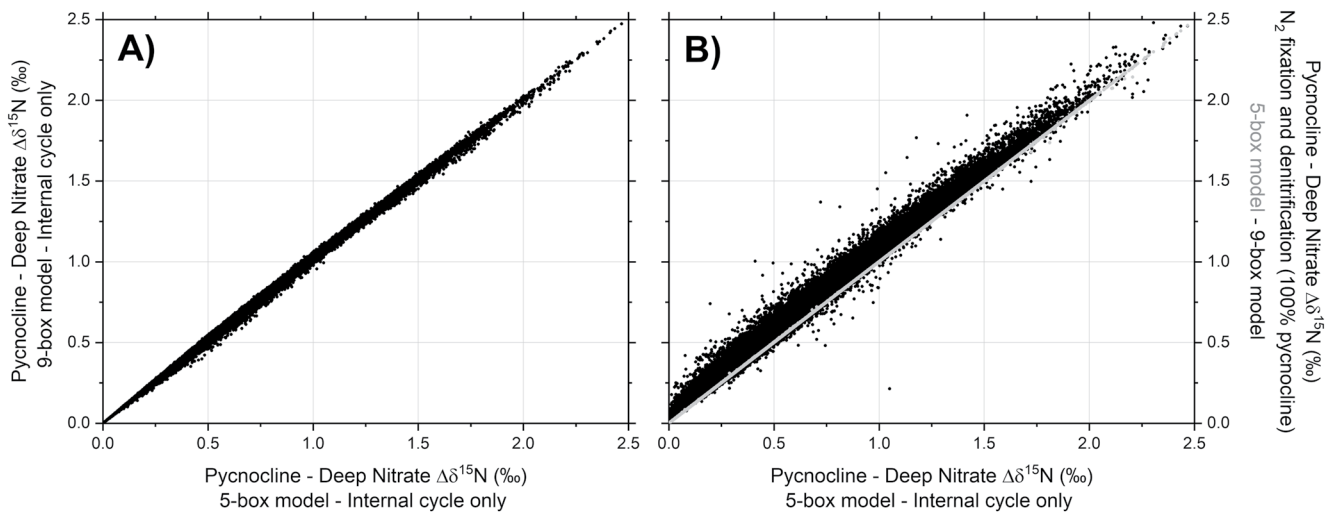
Figure 5.

Figure 6. A comparison of the mean difference in $\delta^{15}N$ ($\Delta\delta^{15}N$) between the pycnocline and the deep ocean between the model configurations with and without N_2 fixation and denitrification. In both panels, the x-axis is the five-box model configuration without N_2 fixation and denitrification (i.e., simulations including only ocean-internal nitrate cycling). In panel (b), the and black circles are for the five-box and nine-box models, respectively. The y-axis in panel (a) is for the model configuration without N_2 fixation and denitrification, and in panel (b) where all N_2 fixation and denitrification occur in the pycnocline. Figure S2 in the Supporting Information S1 includes the model configurations in which a fraction (i.e., 15%) of the addition of newly fixed N and denitrification occur below the pycnocline, and in which the addition of newly fixed N occurs entirely in the pycnocline but a fraction (i.e., 15%) of denitrification (i.e., all as sedimentary denitrification) occurs below the pycnocline.

(Marconi et al., 2019). The isotopic discrimination of nitrate in the upper overturning cell at the Southern Ocean surface yields a positive relationship between pycnocline nitrate $\delta^{15}N$ and the pycnocline recipe (Figure 5c for the five-box model), that is, the fraction of nutrients transported into the pycnocline from the Southern Ocean surface *vs.* the deep ocean (Equation 3). Therefore, in both the five-box and nine-box models, the mean difference in nitrate $\delta^{15}N$ between the pycnocline and the deep ocean ($\Delta\delta^{15}N_{p-d}$) is directly proportional to the pycnocline recipe (Figure 6a).

3.1.2. N_2 Fixation and Denitrification in the Upper Ocean

Superimposed on the internal nitrate cycle, the sources and sinks of fixed N affect the $\delta^{15}N$ of nitrate in the ocean. It has been widely assumed that mean ocean nitrate $\delta^{15}N$ is representative of the budget-driven nitrate $\delta^{15}N$. However, denitrification and N_2 fixation are spatially confined to the upper ocean (Bianchi et al., 2012; Deutsch et al., 2007), and the superposition of the fixed N budget on the meridional overturning circulation (and the resulting fractionation of N isotopes by its upper cell) has received little attention (cf., Marconi et al., 2015; Marconi, Sigman, et al., 2017). In the prognostic models, we tested different treatments of N_2 fixation and denitrification under various degrees to which deep water nutrients return to the pycnocline by Southern Ocean upwelling as opposed to the interior upwelling of deep water (i.e., the pycnocline recipe).

We first assume that denitrification and N_2 fixation are entirely restricted to the pycnocline and the low-latitude surface mixed layer. This is a reasonable assumption given that: (a) N_2 fixation occurs mostly in the low-latitude mixed layer (Deutsch et al., 2007; Luo et al., 2012; Wang et al., 2019) and introduces new nitrate to the pycnocline largely through low-latitude export production and its remineralization within the pycnocline (Gruber & Sarmiento, 1997); (b) most water column denitrification occurs in the suboxic zones, which are also located

Figure 5. The Southern Ocean's impact on the nitrate concentration and $\delta^{15}N$ of the pycnocline and deep ocean. In the five-box ocean model, (a, c, e) the effect of the Southern Ocean versus the deep ocean in the gross nutrient supply to the pycnocline (i.e., the "pycnocline recipe"; Equation 3), and (b, d, f) the effect of the degree of nitrate consumption in Southern Ocean surface waters. Panels (c, d) are for the model scenario without N_2 fixation and denitrification, and panels (e, f) are for the model scenario in which all N_2 fixation and denitrification occur in the pycnocline and the overlying surface. In panels (a, c, e), there is a constant degree of nitrate consumption in the Southern Ocean surface waters, which is set to modern conditions. In panels (b, d, f), there is a constant degree to which deep water returns to the pycnocline by Southern Ocean upwelling as opposed to directly from the deep ocean (i.e., the "overturning ratio"; Equation 4), which is set to the value derived by Fripiat, Martínez-García, et al. (2021) for the modern conditions. The solid lines are for the optimized model scenario (Table 1) with the values of the model parameters from Fripiat, Martínez-García, et al. (2021). The open circles are the model solutions from the sensitivity test (Table 1). The dark blue lines and circles are for the deep ocean, the petrol lines and circles are for the AZ surface waters, the olive lines and circles are for the combined PFZ-SAZ ventilating area, the cyan lines and circles are for the global pycnocline, and the black lines and circles are for the difference between budget-driven nitrate $\delta^{15}N$ and mean ocean nitrate $\delta^{15}N$.
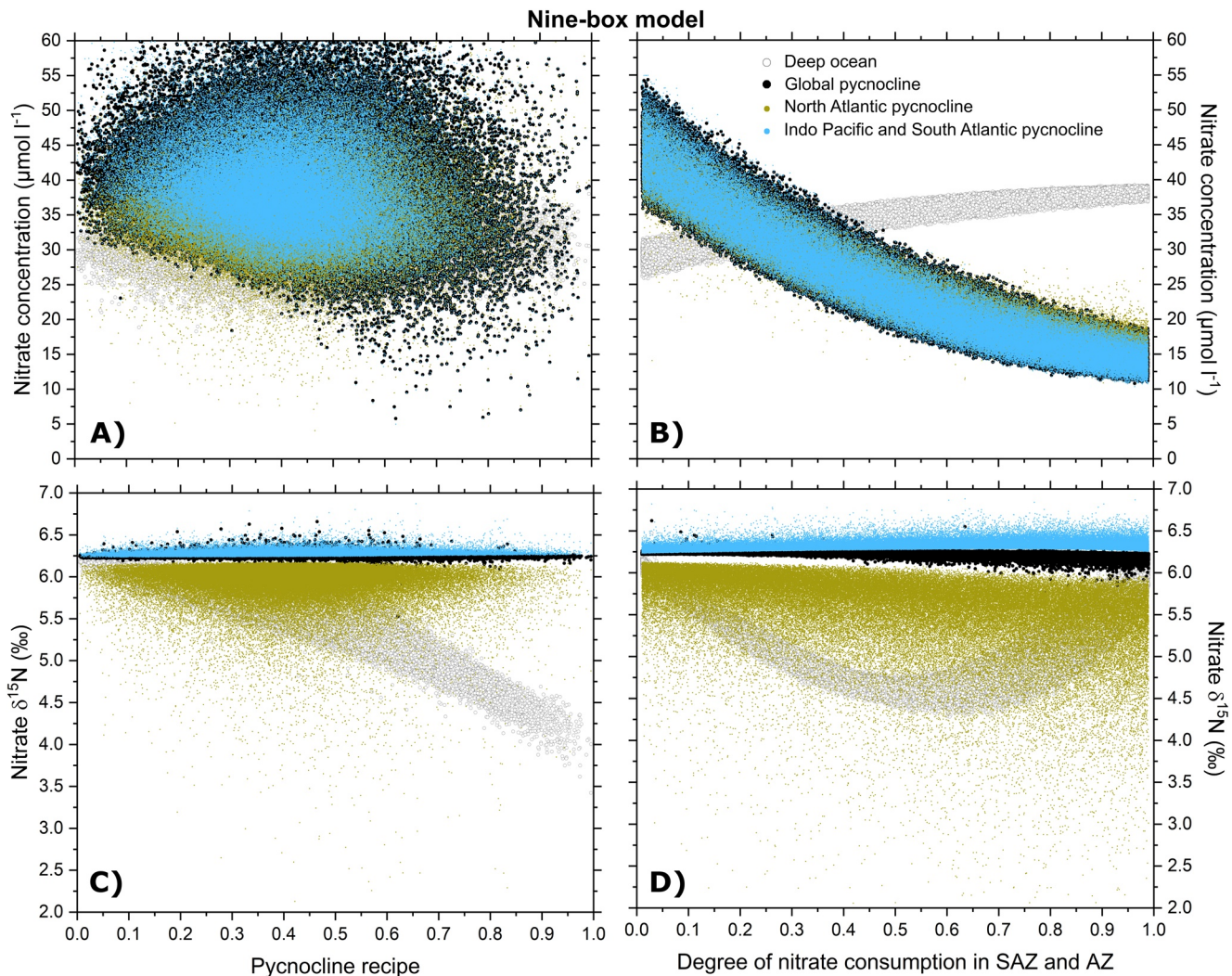
Figure 7. Southern Ocean's impact on the nitrate concentration and $\delta^{15}N$ of the deep ocean and the pycnocline in the prognostic nine-box ocean model in the scenario where all N_2 fixation and denitrification occur in the pycnocline. In (a, c), these are plotted as a function of the relative importance of the Southern Ocean *vs.* the deep ocean in the gross nutrient supply to the pycnocline (i.e., pycnocline recipe; Equation 3), and in (b, d) as a function of the degree of nitrate consumption in Southern Ocean surface waters. In panels (a, c), there is a constant degree of nitrate consumption in Southern Ocean surface waters, set to modern conditions. In panels (b, d), there is a constant degree to which deep water returns to the pycnocline by Southern Ocean upwelling as opposed to directly from the deep ocean (i.e., a constant overturning ratio, Equation 4), which is set to the value derived by Fripiat, Martínez-García, et al. (2021) for modern conditions. The other model parameters are allowed to vary in the range shown in Table 1 for the sensitivity test, as shown in Figures 6 and 7. The gray open circles are for the deep ocean, the solid black circles for the global pycnocline, the cyan circles for the combined Indo-Pacific and South-Atlantic pycnocline, and the olive circles for the North Atlantic pycnocline.

within the pycnocline (Bianchi et al., 2012); and (c) the bulk of sedimentary denitrification occurs on the seafloor at depths within the pycnocline or the overlying surface mixed layer (Bianchi et al., 2012). The low-latitude mixed layer receives its nutrients from the pycnocline, and these nutrients are fully consumed there and returned to the subsurface in sinking organic matter. Thus, N budget fluxes occurring in the low-latitude mixed layer are reflected dominantly in the model's pycnocline. In the supplementary information (Text S2 in Supporting Information S1), we test whether the inclusion of sedimentary denitrification in the deep ocean significantly changes the systematics described below (Bianchi et al., 2012; Middelburg et al., 1996; DeVries et al., 2013). The major finding in this regard is that modest violations of the assumption have little effect (Figures S1 and S2 in Supporting Information S1). Accordingly, the key lessons of our study, based on the conceptually simple case of a fixed N budget contained entirely within the pycnocline, hold more broadly.

For the five-box model, this scenario implies that N_2 fixation and denitrification are spatially confined to one specific volume (i.e., the global pycnocline), so that pycnocline nitrate $\delta^{15}N$ must be forced to the budget-driven
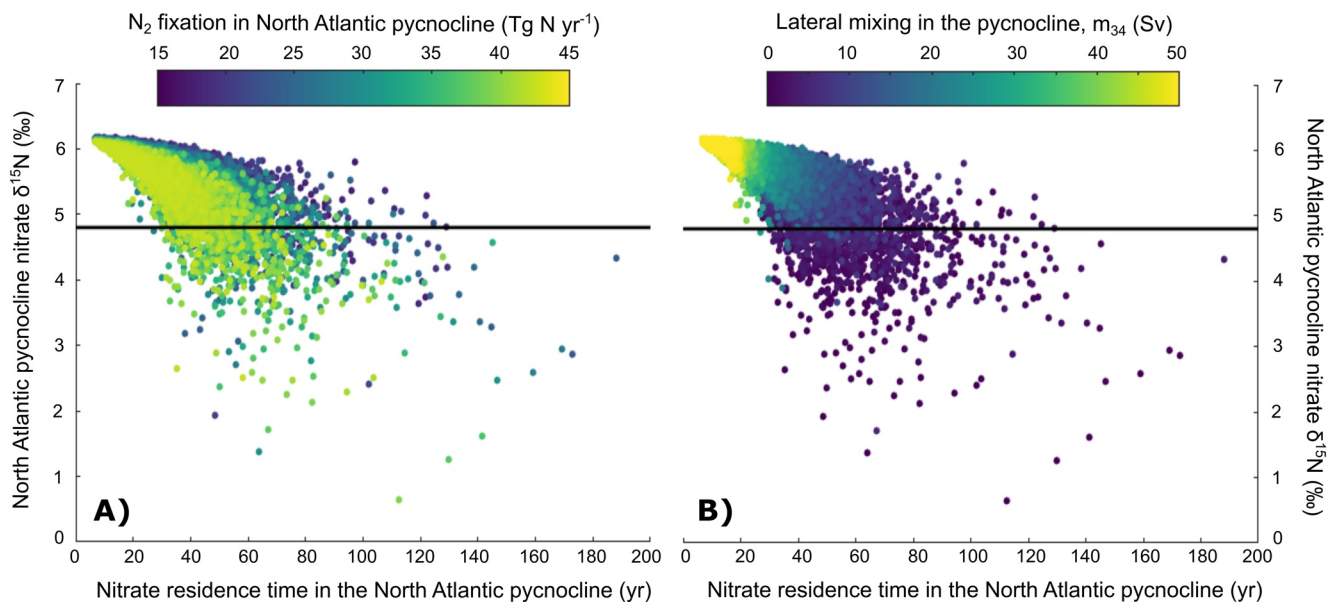
Figure 8. North Atlantic pycnocline nitrate $\delta^{15}N$ versus the residence time of nitrate in the North Atlantic pycnocline in the prognostic nine-box ocean model. The residence time is with respect to the nitrate pool in the pycnocline plus overlying surface; it is not with regard to ventilation at the ocean surface. The color scale in (a) is for the rate of N_2 fixation in the North Atlantic pycnocline (in Tg N yr^{-1}), and the color scale in (b) is for the lateral mixing between the North Atlantic pycnocline and the non-North Atlantic pycnocline (in Sv). The horizontal line represents the observation-based concentration-weighted nitrate $\delta^{15}N$ of the North Atlantic pycnocline (Table S1 in Supporting Information S1).

nitrate $\delta^{15}N$ (= N_2 fixation $\delta^{15}N$ + the net isotopic discrimination by fixed N loss) (Figure 1b). A benefit of this result is that the net isotope effect for denitrification (ε_{deni}) can be estimated from the difference in $\delta^{15}N$ between the observation-based weighted average for the pycnocline (Fripiat, Martínez-García, et al., 2021) and newly fixed N (i.e., ε_{deni} = 6.25‰ − −1‰, or 7.25‰). For the nine-box model, we must define ε_{deni} for the different pycnocline volumes by considering how the ratio between water column and sedimentary denitrification is changing. Given the absence of water column denitrification in the North Atlantic pycnocline, ε_{deni} is set by the isotope effect of sedimentary denitrification (simplified here to be 0‰; Brandes & Devol, 1997; Lehmann et al., 2004, 2007), yielding a budget-driven nitrate $\delta^{15}N$ equivalent to the fixed N input (i.e., −1‰). This result implies that water column denitrification is spatially confined to the remaining pycnocline, yielding a higher ratio between water column and sedimentary denitrification and, therefore, a higher ε_{deni} for this volume. To define its value, we find the best agreement between the optimized model scenario and the observation-based weighted $\delta^{15}N$ averages for the pycnocline and the deep ocean of Fripiat, Martínez-García, et al. (2021) (Figure S1 in Supporting Information S1). This exercise yields a ε_{deni} of ~8.0‰, consistent with a higher ratio between water column and sedimentary denitrification in the non-North Atlantic pycnocline than in the pycnocline as a whole (Bianchi et al., 2012).

We first discuss the results for the five-box model. As for the scenario considering only internal nitrate cycling, a higher value for the pycnocline recipe induces a stronger fractionation of the N isotopes between the deep ocean and the pycnocline (Figures 5c and 5e); the amplitude of this difference is not affected by whether the fixed N budget is included in the model (Figure 6b and Figure S1c in Supporting Information S1). However, with the fixed N budget active, it is a natural outcome of the model that the pycnocline nitrate $\delta^{15}N$ is constantly pushed toward the value required by the fixed N budget (i.e., the budget-driven nitrate $\delta^{15}N$). The response is, therefore, mostly observed in the $\delta^{15}N$ of nitrate in the deep ocean (Figure 5e). Thus, with the fixed N budget active, the net effect of the Southern Ocean's upper cell is almost entirely to lower the $\delta^{15}N$ of nitrate in the deep ocean below the budget-driven nitrate $\delta^{15}N$. Therefore, a higher pycnocline recipe imposes a lower $\delta^{15}N$ for deep ocean and mean ocean nitrate than would apply to a hypothetical homogenous ocean nitrate reservoir with the same input/output fixed N budget (Brandes & Devol, 2002). Since there is no discrimination between the N isotopes during the transport of nitrate from the deep ocean to the pycnocline by interior upwelling, a lower value for the pycnocline recipe causes deep ocean nitrate $\delta^{15}N$ to be closer to the pycnocline nitrate $\delta^{15}N$ and thus to the budget-driven nitrate $\delta^{15}N$ (Figure 5e). In this sense, a low value for the pycnocline recipe yields a mean ocean nitrate $\delta^{15}N$ more in line with previous expectations (Brandes & Devol, 2002).

These systematics also prevail in the nine-box model (Figure 7c), which takes into account an excess of N_2 fixation over denitrification in the North Atlantic Ocean and a near-absence of water column denitrification in this basin (Bianchi et al., 2012; Deutsch et al., 2007; Wang et al., 2019). A higher ratio between water column and sedimentary denitrification in the combined Indo-Pacific and South Atlantic pycnocline leads to a slightly higher nitrate $\delta^{15}N$ than in the global pycnocline, which is compensated by a much larger decrease in $\delta^{15}N$ in the North Atlantic pycnocline (Figure 7c). Nitrate $\delta^{15}N$ in the North Atlantic is mostly a function of the nitrate residence time and N_2 fixation rate in this area (Figure 8a). A higher nitrate residence time in the North Atlantic forces nitrate $\delta^{15}N$ to become closer to the budget-driven value (i.e., $-1‰$), as the North Atlantic pycnocline is more isolated in this case. Nitrate $\delta^{15}N$ in the North Atlantic is also a function of the mixing flux between the two pycnocline domains (m_{34}) for the same reasons (Figure 8b). In this model configuration and independent of the pycnocline recipe, global pycnocline nitrate $\delta^{15}N$ remains close to the budget-driven value at the scale of the pycnocline (Figure 7c), similar to that of the five-box model (Figure 5e). A higher value for the pycnocline recipe induces a stronger fractionation of the N isotopes between the deep ocean and the global pycnocline, with the response mostly observed as a nitrate $\delta^{15}N$ decline in the deep ocean (Figure 7c). In the nine-box model, $\Delta\delta^{15}N_{p-d}$ is shifted slightly higher than in the five-box model (by $+0.07 \pm 0.03‰$; Figure 6b) because of a slightly lower deep ocean nitrate $\delta^{15}N$ for a given pycnocline recipe. This is caused by the transfer of lower $\delta^{15}N$ nitrate into the interior by the sinking of North Atlantic Deep Water. That said, this effect is limited because of the relatively minor contribution of the northward advective flow (ω_N) and North Atlantic sinking N to the export of N from the pycnocline, in comparison to the mixing fluxes and low-latitude export production occurring outside of the North Atlantic. The effect is also counteracted by the higher $\delta^{15}N$ of nitrate and sinking N that transfers N from the non-North Atlantic pycnocline to the deep ocean, caused by a higher ratio of water column to sedimentary denitrification in the non-North Atlantic pycnocline. A similar difference in $\Delta\delta^{15}N_{p-d}$ between the nine-box and five-box models is reported if we consider only the model runs for which nitrate concentration and $\delta^{15}N$ in the North Atlantic match with the observations ($+0.05 \pm 0.05‰$; Table S1 in Supporting Information S1).

The degree of nitrate consumption in Southern Ocean surface waters plays a role in the fractionation of N isotopes between the deep ocean and the pycnocline, influencing the pycnocline recipe and affecting nitrate $\delta^{15}N$ by means of the aforementioned processes (Figures 4, 5c, 5e, and 7c). However, the degree of nitrate consumption also has an influence in itself (Figure 4) as follows. A very low degree of nitrate consumption causes little nitrate $\delta^{15}N$ elevation in Southern Ocean surface waters. In this scenario, the water that enters the pycnocline by subduction carries nitrate with a concentration and $\delta^{15}N$ close to those of the deep ocean (Figure 5b). This results in a situation similar to the transport of nitrate directly from the deep ocean, which occurs with no fractionation. At the other extreme, a very high degree of nitrate consumption results in little nitrate being transferred from the Southern Ocean to the pycnocline and therefore a low pycnocline recipe (Figure 5b). In this case, most of the nitrate in the pycnocline is supplied from the deep ocean, again with no discrimination between the N isotopes. These two end-member scenarios both yield low $\Delta\delta^{15}N_{p-d}$ (Figures 5d and 5f). The highest $\Delta\delta^{15}N_{p-d}$ occurs at an intermediate degree of nitrate consumption (Figures 4b, 5d and 5f). An intermediate degree of nitrate consumption results in both a significant amount of nitrate being present in the subducting waters and an elevated $\delta^{15}N$ for this nitrate due to partial nitrate assimilation in the Southern Ocean surface. A higher $\Delta\delta^{15}N_{p-d}$ lowers the $\delta^{15}N$ of nitrate in the deep ocean (Figures 5d and 5f). In model simulations with the internal nitrate cycle alone, pycnocline nitrate $\delta^{15}N$ is simultaneously elevated (Figure 5d). However, in simulations in which N_2 fixation and denitrification are included, pycnocline nitrate $\delta^{15}N$ is controlled dominantly by the fixed N budget and is thus very close to the budget-driven nitrate $\delta^{15}N$ (Figure 5f). In these simulations, the high $\Delta\delta^{15}N_{p-d}$ results nearly completely from the lowering of the $\delta^{15}N$ of nitrate in the deep ocean.

These systematics are also observed in the nine-box model (Figure 7d and Figure S1b in Supporting Information S1) but with $\Delta\delta^{15}N_{p-d}$ shifted toward slightly higher values (Figure 6b). This slight increase in $\Delta\delta^{15}N_{p-d}$ due to the separation of the Indo-Pacific from the North Atlantic is a consequence of North Atlantic processes mimicking an isotopic fractionation in the nitrate transport associated with North Atlantic Deep Water formation: the $\delta^{15}N$ of nitrate being fed into the deep ocean from the North Atlantic pycnocline is lower than the $\delta^{15}N$ of global mean pycnocline nitrate.

To summarize, we have identified three key dynamics that determine the Southern Ocean's impact on mean ocean nitrate $\delta^{15}N$. First, the mean difference in nitrate $\delta^{15}N$ between the pycnocline and the deep ocean ($\Delta\delta^{15}N_{p-d}$) is directly proportional to the pycnocline recipe for a given degree of nitrate consumption in the Southern Ocean (Figures 4, 5, 7 and 9). Second, for a given pycnocline recipe, an intermediate degree of Southern Ocean nitrate
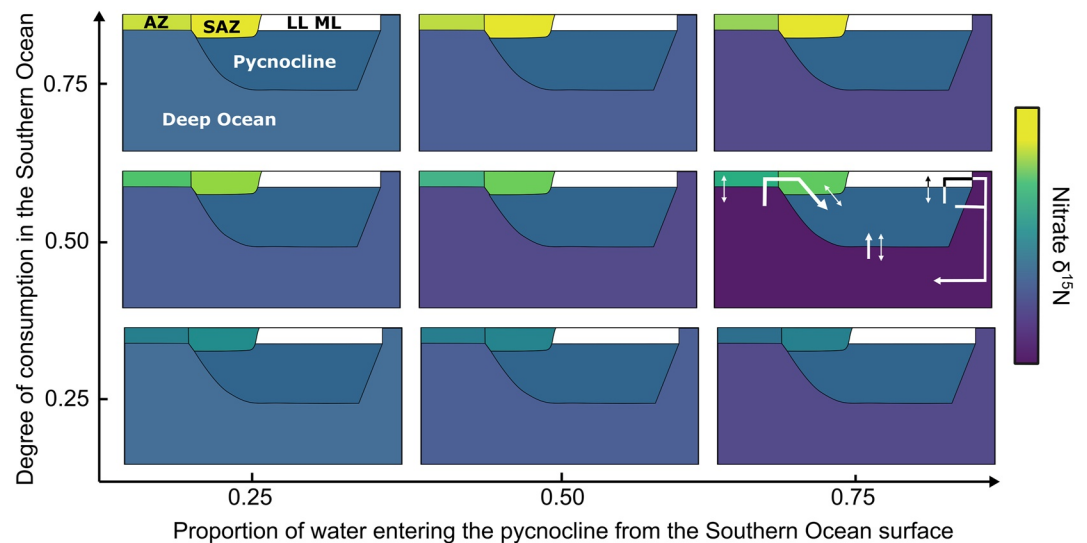
Figure 9. The nitrate $\delta^{15}N$ distribution in the five-box model (Figure 3a) as a function of the proportion of water that enters the pycnocline from the Southern Ocean surface (*x*-axis) and the degree of nitrate consumption in the Southern Ocean surface (*y*-axis) according to the systematics described in this study (Figures 5e and 5f). In these model runs, the ocean's fixed N budget is assumed to operate entirely through the pycnocline and overlying surface waters, such that the pycnocline nitrate $\delta^{15}N$ holds constant. The greatest nitrate $\delta^{15}N$ difference between the pycnocline and the deep ocean and thus the lowest $\delta^{15}N$ for deep and mean ocean nitrate occur under an intermediate degree of Southern Ocean nitrate consumption and a high proportion of flow through the Southern Ocean surface. Abbreviations are as follows: AZ, Antarctic Zone; SAZ, Subantarctic Zone; LL ML, low latitude mixed layer.

consumption yields a higher $\Delta\delta^{15}N_{p-d}$ than either very low or very high degrees of consumption do. Third, the ocean's fixed N budget keeps the pycnocline nitrate $\delta^{15}N$ close to the budget-driven nitrate $\delta^{15}N$ (Figures 5e, 5f, 7c, 7d and 9). Thus, the Southern Ocean causes the $\delta^{15}N$ of deep ocean and mean ocean nitrate to deviate from (i.e., be lower than) the budget-driven nitrate $\delta^{15}N$ by an amplitude that is proportional to the pycnocline recipe and that also varies with the degree of nitrate consumption in Southern Ocean waters.

We acknowledge that our prognostic multi-box ocean model is a simplification of the real ocean, focusing on the Southern Ocean's upper cell, and that other processes are not dynamically tested. For example, we do not explicitly resolve intermediate and deep water masses, and N_2 fixation and denitrification are not spatially resolved in the different boxes. With the conceptual framework established here, the same dynamics should be investigated in more spatially revolved N isotope models (e.g., Buchanan et al., 2019; DeVries et al., 2013; Somes et al., 2013; Yang & Gruber, 2016).

3.2. Implications for the Pycnocline Recipe

Fripiat, Martínez-García, et al. (2021) used a steady-state model for the pycnocline and a large-scale nitrate isotope data compilation to place observational constraints on the pycnocline recipe (Equation 3). The rationale involved using the positive relationship between the pycnocline recipe and the mean difference in $\delta^{15}N$ between the pycnocline and the deep ocean (i.e., $\Delta\delta^{15}N_{p-d}$; Figures 5 and 7). The model equations were solved by varying the model parameters and targeting the best agreement between the observations and the model counterparts (i.e., control run in Figure 10). The control run corresponded to the model configuration of the five-box model where all N_2 fixation and denitrification occur in the pycnocline (Figure 6b). The best fits for the pycnocline recipe had a median of 0.61 (0.56–0.68, 10th and 90th percentile).

In the five-box model, we assume that isotopic gradients across the pycnocline are small and that there is no spatial correlation between cross-pycnocline transports and the nitrate concentration and $\delta^{15}N$ gradients between the pycnocline and the underlying deep ocean. The strongest real-world exception to this involves the North Atlantic, where low-$\delta^{15}N$ nitrate is transferred into the ocean interior by the sinking of North Atlantic Deep Water (i.e., ω_N). Using a nine-box model which now captures this dynamic (Figures 2c and 3b), we show that
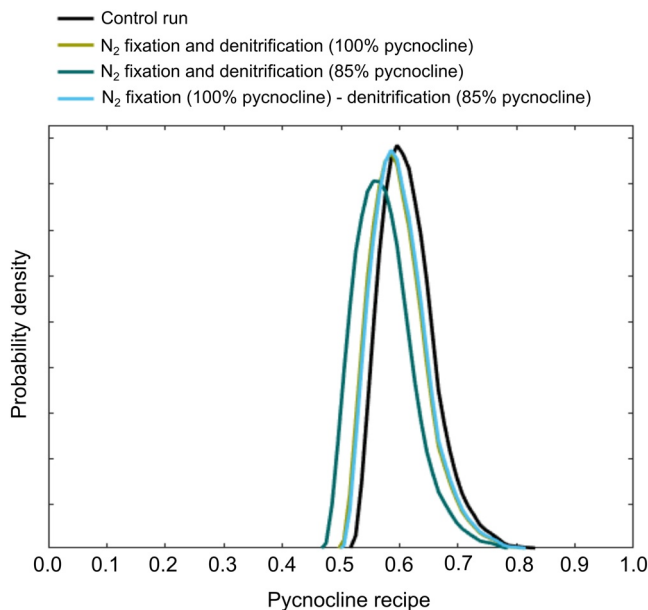
Figure 10. The density function of the model best fits for the pycnocline recipe, based on the steady-state, one-box model developed in Fripiat, Martínez-García, et al. (2021). The black line is the distribution of model best fits from the control run in Fripiat, Martínez-García, et al. (2021), corresponding to the five-box model and the model configuration where all addition of newly fixed N and denitrification occur in the pycnocline (Figure 6b). To capture the various treatments of N₂ fixation and denitrification in the nine-box model, we rerun the one-box model after applying the offset in $\Delta\delta^{15}N_{p-d}$ from the five-box model with the fixed N budget of the control run. The olive line is for the nine-box model configuration where all N₂ fixation and denitrification occur in the pycnocline (Figure 6b), the petrol line for the nine-box model configuration where a fraction (i.e., 15%) of N₂ fixation and denitrification occurs outside the pycnocline (Figure S2c in Supporting Information S1), and the cyan line for the nine-box model configuration where all N₂ fixation occurs in the pycnocline but a fraction (i.e., 15%) of denitrification occurs outside the pycnocline (Figure S2d in Supporting Information S1). Any denitrification in the deep boxes is sedimentary denitrification, occurring without isotopic fractionation.

it plays a minor but quantifiable role in $\Delta\delta^{15}N_{p-d}$ (Figure 6). Here, we evaluate its impact on the estimates of the pycnocline recipe given by Fripiat, Martínez-García, et al. (2021).

In order to do so, we correct $\Delta\delta^{15}N_{p-d}$ calculated in Fripiat, Martínez-García, et al. (2021) for the mean differences among the different model configurations observed here (Figure 6). Our estimate for the pycnocline recipe is slightly lower than but not significantly different from that reported in Fripiat, Martínez-García, et al. (2021) (Figure 10; Table 2): a median for the best fits of 0.59 (0.54–0.66, 10th and 90th percentile) for the nine-box model scenario where all N₂ fixation and denitrification occur in the pycnocline, 0.57 (0.52–0.64) where a fraction (i.e., 15%) of N₂ fixation and denitrification (i.e., all as sedimentary denitrification) occurs outside the pycnocline, and 0.60 (0.55–0.67) where all N₂ fixation occurs in the pycnocline but a fraction (i.e., 15%) of denitrification (i.e., all as sedimentary denitrification) occurs outside the pycnocline (see Text S2 in Supporting Information S1 for a description of these scenarios).

These differences are minor. However, they all point to a lower pycnocline recipe than that estimated by Fripiat, Martínez-García, et al. (2021). In turn, the estimate of Fripiat, Martínez-García, et al. (2021) was modestly lower than widely cited prior estimates, for example, 0.75 from Sarmiento et al. (2004). Thus, the N isotopes appear to point to a greater role for directly supplied deep water nitrate in the pycnocline than has been the recent consensus, in which the Southern Ocean input is often framed as overwhelmingly important. While this is an important finding, its nuances should be appreciated. In particular, the estimate of Fripiat, Martínez-García, et al. (2021) and our calculations here refer to the entire depth range of the pycnocline, whereas the shallow pycnocline is the most direct nutrient source to the low-latitude surface, and it likely contains a lower proportion of directly supplied deep nitrate than is reflected by the whole-pycnocline average.

3.3. Implications for the Ocean's Fixed N Budget

Nitrate $\delta^{15}N$ provides an integrative geochemical tool for constraining the removal of fixed N from the ocean (Altabet, 2007; Brandes & Devol, 2002; Deutsch et al., 2004; DeVries et al., 2013; Eugster & Gruber, 2012; Sigman et al., 2009; Somes et al., 2013). The rationale involves the use of the difference in expressed isotope discrimination between sedimentary and water column denitrification, the latter being largely responsible for elevating nitrate $\delta^{15}N$ relative to the fixed N input. The net discrimination associated with

Table 2
Estimates of the Model Best Fits for the Pycnocline Recipe, Based on the Steady-State, One-Box Model Developed in Fripiat, Martínez-García, et al. (2021)

Pycnocline recipe Model configurations	Average ± SD	Median	10th percentile	90th percentile
Control run (five-box model; N₂ fix./deni. 100% pycnocline)	0.62 ± 0.05	0.61	0.56	0.68
Nine-box model: N₂ fix./deni. 100% pycnocline	0.60 ± 0.05	0.59	0.54	0.66
Nine-box model: N₂ fix./deni. 85% pycnocline	0.58 ± 0.05	0.57	0.52	0.64
Nine-box model: N₂ fix. 100% pycnocline/deni. 85% pycnocline	0.60 ± 0.05	0.60	0.55	0.67

Note. To capture the various treatments of N₂ fixation and denitrification in the nine-box model, we rerun the one-box model after having applied the offset in $\Delta\delta^{15}N_{p-d}$ from the Five-Box Model with the fixed N budget of the control run. The density function of the model best fits is shown in Figure 10.

denitrification ($\varepsilon_{\text{deni}}$) combines the isotope effects of water column (ε_{wcd}) and sedimentary denitrification (ε_{sd}), as follows:

$$\varepsilon_{\text{deni}} = X_{\text{wcd}} \cdot \varepsilon_{\text{wcd}} + X_{\text{sd}} \cdot \varepsilon_{\text{sd}} \tag{5}$$

where X_{wcd} and X_{sd} are the fractional contributions of water column and sedimentary denitrification to total denitrification (Brandes & Devol, 2002; Marconi, Kopf, et al., 2017). Previous studies specifically used mean ocean nitrate δ^{15}N (~5.0‰) as being representative of the budget-driven nitrate δ^{15}N. Our study shows that mean ocean nitrate δ^{15}N is lower than the budget-driven nitrate δ^{15}N, due to: (a) the high degree to which deep water returns to the pycnocline by wind-driven upwelling in the Southern Ocean (Gnanadesikan et al., 2007; Marshall & Speer, 2012; Sarmiento et al., 2004) and (b) partial nitrate assimilation in Southern Ocean surface waters, which leads to a fractionation of N isotopes between the deep and upper oceans (Figure 2) (Sigman et al., 2000, 2009). In addition, our study also shows that pycnocline nitrate δ^{15}N (~6.25‰) is very similar to the budget-driven nitrate δ^{15}N since most N$_2$ fixation and denitrification are confined to the upper ocean (Bianchi et al., 2012). This implies a higher budget-driven nitrate δ^{15}N than if the mean ocean nitrate δ^{15}N is applied to Equation 5 and, thus, a higher ratio of water column to sedimentary denitrification for a given mean ocean nitrate δ^{15}N.

To evaluate the effect of these considerations on denitrification rate estimates, we solve Equation 5 by assuming either mean ocean nitrate δ^{15}N or pycnocline nitrate δ^{15}N as being representative of the budget-driven nitrate δ^{15}N (Table 3). We also consider a scenario where 20% of sedimentary denitrification occurs outside the pycnocline in the deep ocean (see Text S2 in Supporting Information S1) and the nine-box model configuration where all N$_2$ fixation and denitrification occur in the pycnocline but with two separate boxes for the pycnocline (non-North Atlantic and North Atlantic). The δ^{15}N of N$_2$ fixation is set to −1‰, yielding a $\varepsilon_{\text{deni}}$ of 6.0, 7.25, 8.3, and 8.0‰ respectively. For the nine-box model, this value is representative of the non-North Atlantic pycnocline, where 100% of water column denitrification and 90% of total denitrification occur. In order to solve Equation 5, we must also define the isotope effects for water column and sedimentary denitrification, as well as for the δ^{15}N of newly fixed N. These terms are still being refined (e.g., Marconi, Kopf, et al., 2017; Martin et al., 2019; McRose et al., 2019). We consider both low and high estimates for the isotope effect of water column denitrification (i.e., 13 and 25‰, respectively; Brandes et al., 1998; Barford et al., 1999; Casciotti et al., 2013; Kritee et al., 2012; Marconi, Kopf, et al., 2017; Sigman et al., 2005; Voss et al., 2001). Other processes (e.g., nitrite oxidation, anammox) also appear to impact the net isotope effect of water column N loss (Brunner et al., 2013; Casciotti et al., 2013; Martin et al., 2019; Sigman et al., 2005); we do not include these processes here. The isotope effect for sedimentary denitrification is set to 0‰ (Table 2), despite evidence for higher values in specific systems (Alkhatib et al., 2012; Brandes & Devol, 1997; Fripiat et al., 2018; Granger et al., 2011; Lehmann et al., 2004, 2007). Our goal is not to distinguish between these values but rather to quantify the impact of Southern Ocean circulation and nitrate consumption on the N isotope budget.

Taking the pycnocline nitrate δ^{15}N as representative of the budget-driven nitrate δ^{15}N increases the ratio of water column to sedimentary denitrification by 10%–40% and lowers the total denitrification rate by 25–50 Tg N yr^{-1}, relative to the assumption of mean ocean nitrate δ^{15}N as representative of the budget-driven nitrate δ^{15}N (Table 3). Although significant, this effect is limited compared to the role of the magnitude of the isotope effect for water column denitrification (i.e., 13 *vs.* 25‰): the lower isotope effect increases the ratio of water column to sedimentary denitrification by 55%–85% and decreases the calculated total denitrification rate by 115–140 Tg N yr^{-1} (Deutsch et al., 2004; Marconi, Kopf, et al., 2017). The inclusion of sedimentary denitrification outside the pycnocline and/or the separation of the pycnocline into North Atlantic and non-North Atlantic volumes do not have major additional effects (Table 3).

In summary, our study highlights that the nitrate δ^{15}N of the pycnocline, not of the deep ocean or global mean ocean, best represents the budget-driven nitrate δ^{15}N. This implies a greater contribution of water column denitrification to the removal of fixed N from the ocean and reduces the previously identified deficit of N inputs relative to N losses, although only modestly (Table 3). Spatially resolved and multi-box δ^{15}N models tend to yield a higher ratio of water column to sedimentary denitrification (DeVries et al., 2013; Eugster & Gruber, 2012; Somes et al., 2013). This is at least partially due to the simulation of restricted regions of water column denitrification in which nitrate is consumed to significant degrees, yielding the "dilution effect" (Deutsch et al., 2004). However, the impact of Southern Ocean circulation and nitrate consumption on the N isotope budget, which spatially resolved and multi-box models of the N cycle implicitly capture, may be an important additional cause.

Table 3

Ocean Fixed N Budget Under Different Assumptions: (a) Mean Ocean or Pycnocline Nitrate δ15N as Representative of the Budget-Driven Nitrate δ15N; (b) End-Members for the Isotope Effects of Water Column Denitrification; (c) Various Model Configurations (Figure S2c in Supporting Information S1)

Budget-driven nitrate δ^{15}N	Mean ocean		Pycnocline		Fraction of sed. denitrification in the deep ocean*		Pycnocline (nine-box model)**	
$\varepsilon_{\mathbf{wcd}}$ (‰)	25	13	25	13	25	13	25	13
ε_{sd} (‰)	0	0	0	0	0	0	0	0
Water column denitrification[a] (Tg N yr^{-1})	70	70	70	70	70	70	70	70
N$_2$ fixation δ^{15}N[b] (‰)	−1	−1	−1	−1	−1	−1	−1	−1
$\varepsilon_{\mathbf{deni}}$ (‰) = Budget-driven nitrate δ^{15}N–N$_2$ fixation δ^{15}N	6.00	6.00	7.25	7.25	8.30	8.30	8.00	8.00
Water column to total denitrification ratio	0.24	0.46	0.29	0.56	0.28	0.59	0.29	0.55
Water column to sedimentary denitrification ratio	0.32	0.86	0.41	1.26	0.40	1.41	0.40	1.24
Sedimentary denitrification (Tg N yr^{-1})—pycnocline			171	56	141	40	173	56
Total denitrification (Tg N yr^{-1})—pycnocline			241	126	211	110	243	126
Sed. denitrification (Tg N yr^{-1})—Indo-Pacific-South Atlantic pycnocline							149	44
Total denitrification (Tg N yr^{-1})—Indo-Pacific-South Atlantic pycnocline							219	114
Sedimentary denitrification (Tg N yr^{-1})—total	222	82	171	56	176	50	173	56
Total denitrification (Tg N yr^{-1})	292	152	241	126	246	120	243	126
Total N$_2$ fixation[c] (Tg N yr^{-1})	90–230		90–230		90–230		90–230	

[a]Bianchi et al. (2012), DeVries et al. (2012, 2013), Wang et al. (2019).

[b]Minagawa and Wada (1986), Carpenter et al. (1997), McRose et al. (2019).

[c]Deutsch et al. (2007), Eugster and Gruber (2012), Wang et al. (2019).

* for the Inclusion of Sedimentary Denitrification in the Deep Ocean, i.e., 20% of the Total; ** for the Nine-Box Model Configuration Where all N$_2$ Fixation and Denitrification Occur in the Pycnocline.

3.4. Paleoceanographic Implications

It is often assumed that any change in deep ocean nitrate δ^{15}N must be the result of changes in the fixed N budget (Brandes & Devol, 2002; Deutsch et al., 2004; Galbraith et al., 2013; Kienast, 2000). In contrast, our study shows that deep ocean nitrate δ^{15}N is also sensitive to the pycnocline recipe and the degree of nitrate consumption in Southern Ocean surface waters (Figures 5 and 7). Conversely, one might expect that the δ^{15}N of nitrate in the pycnocline as a whole should respond to changes in Southern Ocean nutrient dynamics; yet, we have shown that, at a steady state, pycnocline nitrate δ^{15}N is dominantly set by the fixed N budget. These findings have implications for the interpretation of paleoceanographic N isotope records.

3.4.1. Southern Ocean Nutrient Conditions During the Ice Ages

Across the Southern Ocean, the δ^{15}N of organic matter bound in the fossils of diatoms, planktic foraminifera, and deep sea corals was ~4‰ higher during the Last Glacial Maximum relative to the Holocene. This suggests a more complete nitrate consumption in surface waters, supporting a key role for the Southern Ocean in ice age reductions in atmospheric CO$_2$ (Ai et al., 2020; Martínez-García et al., 2014; Robinson & Sigman, 2008; Studer et al., 2015; Wang et al., 2017). In the AZ specifically, a higher degree of nitrate consumption coincides with evidence from proxies for a lower rate of export production (Anderson et al., 2009; François et al., 1997; Jaccard et al., 2013; Kumar et al., 1993; Mortlock et al., 1991). These two changes together point to a lower gross nitrate supply to the surface and thus an apparent ice age reduction in the exchange of water between the surface and the underlying ocean (Ai et al., 2020; François et al., 1997). In order to match paleo-biogeochemical proxies during ice ages (i.e., fossil-bound δ^{15}N and export production), preliminary reconstructions of the degree of nitrate consumption alone indicate a severe reduction in the rate of gross nitrate supply to the AZ surface, and the estimated reduction is even more extreme (a reduction of more than 80%) when the evidence for a sharp decline in export production is included (Kemeny et al., 2018). Of the existing hypotheses, a slowdown of the upper cell has the best chance of causing such a large reduction in gross nitrate supply (Sigman et al., 2021; Toggweiler et al., 2006). Model simulations of the ice age wind field are ambiguous with regard to their support for an ice age reduction in wind-driven upwelling (e.g., Sime et al., 2013), but no support can be found for a >80% reduction.

A weakening of the upper cell and/or greater degree of nitrate consumption in the Southern Ocean would have decreased the fraction of nutrients transported from the deep ocean to the pycnocline through Southern Ocean surface waters (i.e., a lower pycnocline recipe). According to our steady state model simulations, this would yield a higher $\delta^{15}N$ for nitrate in the deep ocean (Figures 5 and 7), which may explain a fraction (up to ~1‰) of the increase in fossil-bound $\delta^{15}N$ during ice ages. A higher deep-ocean nitrate $\delta^{15}N$ would allow for a weaker decrease in the gross nitrate supply to match the proxy reconstructions. This consideration may allow the proxy data to be explained with an ice age upwelling rate that is plausible from the perspective of model and data constraints on the ice age wind field (Chavaillaz et al., 2013; Kohfeld et al., 2013; Sime et al., 2013).

3.4.2. Deglacial Maxima in Low-Latitude N Isotope Records

A feature that is commonly reported in low-latitude bulk sediment and fossil-bound $\delta^{15}N$ records is the presence of a deglacial peak (Galbraith et al., 2013; Studer et al., 2021, and references therein). This peak has most often been interpreted as the result of a faster increase in water column than sedimentary denitrification during the deglaciation, yielding a transient higher ratio of water column to sedimentary denitrification (e.g., Deutsch et al., 2004). Our steady state model simulations suggest that a deglacial peak in $\delta^{15}N$ might also have been generated as a transient response of the pycnocline nitrate $\delta^{15}N$ to a change in either the degree of nitrate consumption in the Southern Ocean or the degree to which deep water returns to the upper ocean by wind-driven upwelling (i.e., the overturning ratio) (Wang et al., 2017). Depending on the strength and time scale of this signal, it may offer an alternative to modifications of the fixed N budget as the cause of the deglacial $\delta^{15}N$ maximum.

3.4.3. Time-Dependent Model Experiments

To address these possibilities, we run time-dependent model experiments (Figure 11) using the five-box model, starting from hypothesized glacial conditions in the Southern Ocean and shifting to modern conditions. Similar runs were performed using the nine-box model (Figure S4 in Supporting Information S1). The hypothesized glacial conditions include a higher degree of nitrate consumption relative to the modern with or without a lower degree to which deep water returns to the pycnocline by wind-driven upwelling in the Southern Ocean (Sigman et al., 2021, and references therein). Modern conditions are those derived by Fripiat, Martínez-García, et al. (2021), implying a pycnocline recipe of 0.62. The model is run for 20,000 years under glacial conditions to reach a steady state. A perturbation is then applied for 7,000 years, roughly corresponding to the duration of the last deglaciation. The perturbation consists of either (a) a progressive decrease in the degree of nitrate consumption from 0.95 in both the SAZ and AZ to modern conditions (Figures 11a, 11b and Figures S4a, S4b in Supporting Information S1), (b) a progressive increase in the overturning ratio from 0.1 to 0.9 (Figures 11c, 11d and Figurs S4c, S4d in Supporting Information S1), or (c) both (a) and (b) (Figures 11e, 11f and Figures S4e, S4f in Supporting Information S1). The glacial-interglacial changes in the degree of nitrate consumption are inferred from fossil-bound $\delta^{15}N$ records (Martínez-García et al., 2014; Studer et al., 2015; Wang et al., 2017) and Rayleigh fractionation kinetics (e.g., Figure 10 in Fripiat et al., 2019). The glacial-interglacial changes in the overturning ratio are based on a reduction in the Southern Ocean upper overturning cell inferred to explain paleo-biogeochemical proxy data from the ice ages (i.e., those from fossil-bound $\delta^{15}N$ and export production proxies) (Kemeny et al., 2018 and references therein). For each of these simulations, the model parameters associated with N_2 fixation and denitrification are held constant. This includes the budget-driven nitrate $\delta^{15}N$ for the global pycnocline that we set to 6.25‰, corresponding to the steady state model simulations described above in which all N_2 fixation and denitrification occur in the pycnocline (Figures 5e, 5f, 7c, and 7d).

In all simulations, despite a constant input-output budget for global ocean-fixed N, the model produces a deglacial peak in pycnocline nitrate $\delta^{15}N$ (Figure 11 and Figure S4 in Supporting Information S1). Here, we discuss the results for the five-box model; similar results are reported for the nine-box model, except for the slightly (≤0.2‰) lower deep ocean nitrate $\delta^{15}N$, as discussed in Section 3.1, that is caused by the formation of low-$\delta^{15}N$ NADW.

Changes in the degree of nitrate consumption in the Southern Ocean affect the concentration and isotopic composition of nitrate in the water subducted into the pycnocline in the PFZ-SAZ ventilating area. In simulation (a), with high Southern Ocean nitrate consumption during the ice age, the $\delta^{15}N$ of the residual nitrate is strongly elevated, but the water holds little nitrate (Figures 11a and 11b). Thus, the Southern Ocean surface waters subducted into the pycnocline are depleted in nitrate and have little impact on the pycnocline nitrate $\delta^{15}N$. The resulting lower pycnocline recipe therefore imposes less of a difference in nitrate $\delta^{15}N$ between the deep ocean and the pycnocline (Figure 11b). With a decrease in nitrate consumption during the deglaciation, a pulse
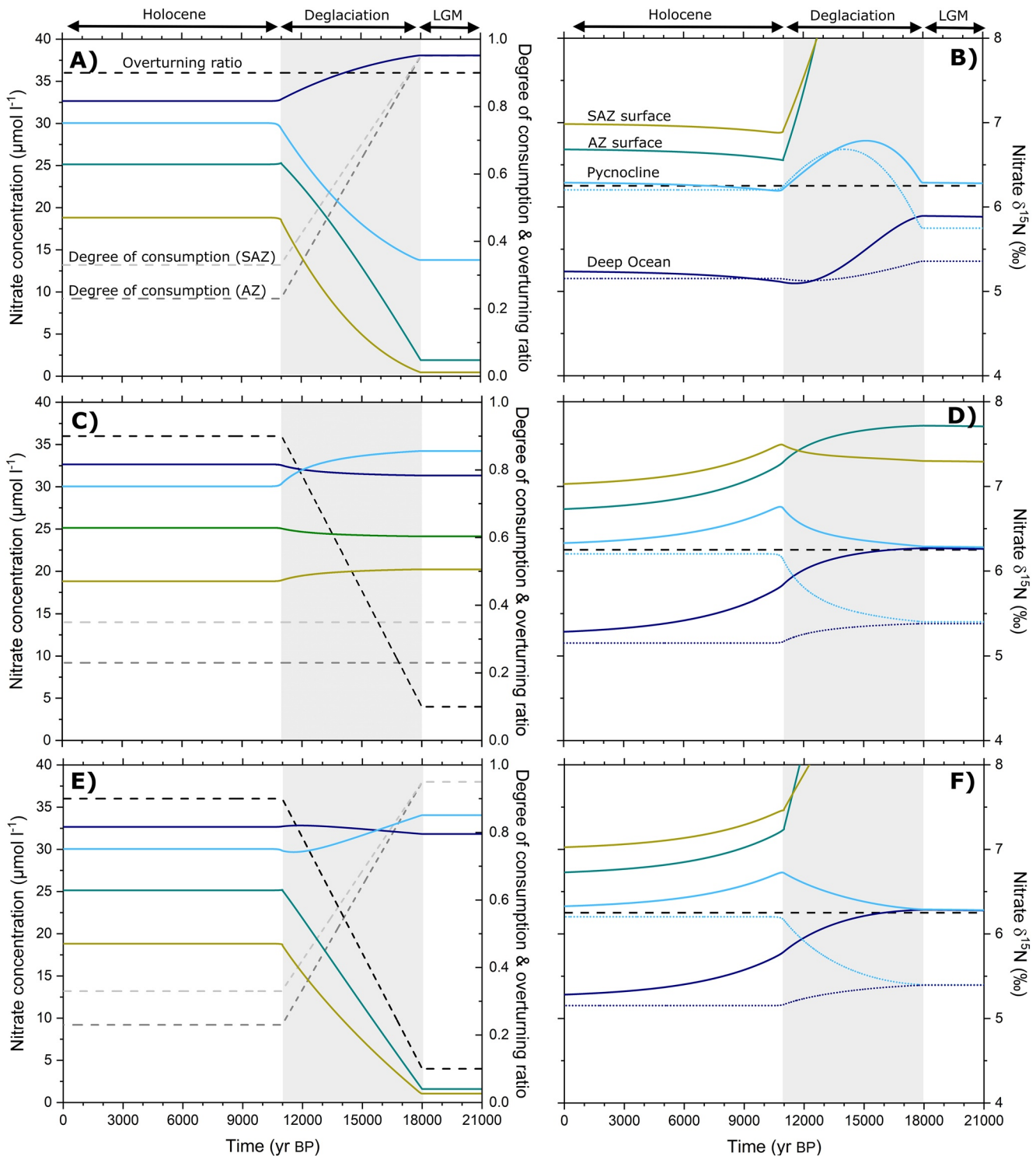
Figure 11.

of residual nitrate with a modestly elevated δ15N but a higher concentration is transferred to the pycnocline, generating a transient increase in its nitrate δ15N. However, pycnocline nitrate δ15N then gradually returns to the budget-driven value at the end of the deglaciation, while the higher pycnocline recipe drives a larger nitrate δ15N difference between the pycnocline and the deep ocean, which equates to a lower deep ocean nitrate δ15N (solid lines in Figure 11b). Comparison with model runs that exclude the fixed N budget suggests that most of the

deglacial peak in pycnocline nitrate $\delta^{15}N$ is driven by the variation in the degree of nitrate consumption during the deglaciation (dotted lines in Figure 11b).

Considering simulation (b) with an increase in the overturning ratio during the deglaciation and simulation (c) with a decrease in Southern Ocean nitrate consumption as well as an increase in the overturning ratio, both simulations generate a deglacial peak in pycnocline nitrate $\delta^{15}N$, of similar amplitude as in simulation (a) (Figures 11d and 11f). However, in simulations (b) and (c), the deglacial peak has a different character from simulation (a), occurring later and decaying more slowly through the simulated interglacial period. Early in the deglaciation, the low overturning ratio in (b) and (c) initially prevents a major impact of Southern Ocean processes (i.e., variation in the degree of nitrate consumption) on pycnocline nitrate $\delta^{15}N$ since most of the nitrate is supplied from the deep by mixing-driven upwelling. Only once the overturning ratio has increased can the Southern Ocean change in nitrate consumption be "felt" by the pycnocline. In effect, then, the later peaks in (b) and (c) delay the deglacial $\delta^{15}N$ maximum in the pycnocline. The pycnocline nitrate $\delta^{15}N$ decline in simulations (b) and (c) after the deglaciation reflects the gradual return of pycnocline nitrate $\delta^{15}N$ to the budget-driven value.

In each of the simulations, deep ocean nitrate $\delta^{15}N$ declines upon deglaciation (Figure 11 and Figure S4 in Supporting Information S1), reflecting the development of the modern isotopic difference from the pycnocline due to the Southern Ocean upper cell and the degree of nitrate consumption therein (Figure 4b). As with the pycnocline nitrate $\delta^{15}N$ changes, the decline in deep ocean nitrate $\delta^{15}N$ is mostly observed during the deglaciation in simulation (a) (Figure 11b and Figure S4 in Supporting Information S1) but continues throughout the simulated interglacial period in simulations (b) and (c) (Figures 11d, 11f and Figure S4d and S4f in Supporting Information S1).

Previous evidence of $\delta^{15}N$ changes during the deglaciation and early Holocene should be revisited in light of our findings (Galbraith et al., 2013; Studer et al., 2018, 2021). Low-latitude records should be sensitive to the nitrate $\delta^{15}N$ of the pycnocline, whereas Southern Ocean and other high-latitude records should be sensitive to the nitrate $\delta^{15}N$ of the deep ocean.

Simulations (b) and (c) with a progressive increase in the overturning ratio generate a deglacial peak in pycnocline nitrate $\delta^{15}N$ that is similar in timing but slightly smaller in magnitude than the average trends inferred from a compilation of bulk sediment $\delta^{15}N$ records in midlatitudes and low latitudes (Figure 12a) (Galbraith et al., 2013). This suggests that the transient response of pycnocline nitrate $\delta^{15}N$ to the changes in Southern Ocean overturning circulation may explain a significant portion ($\sim 0.6‰$) of the observed deglacial and Holocene $\delta^{15}N$ changes ($\sim 0.9‰$). However, much larger deglacial peaks in $\delta^{15}N$ are reported in sedimentary records representative of the OMZs (Hendy & Pedersen, 2006; Higginson & Altabet, 2004; Pichevin et al., 2010; Thunnel & Kepple, 2004), including in fossil-bound $\delta^{15}N$ records (Studer et al., 2021), and with some of them occurring earlier in the deglaciation (i.e., more in line with simulation (a)). While further studies of the sensitivity of the deglacial $\delta^{15}N$ peak to model parameters are required, including of the time scales of the perturbation and response, preliminary experiments suggest that additional processes (such as changes in the fixed N budget) are required to explain the full magnitude and timing of the deglacial and Holocene features in some paleoceanographic records.

Coincidentally, there is a deglacial decline in deep ocean nitrate $\delta^{15}N$, which may have contributed to Southern Ocean N isotope deglacial changes (Ai et al., 2020; Studer et al., 2015), including through the Holocene for simulations with a progressive increase in the overturning ratio (Studer et al., 2018). However, as expected from the steady state results, the total simulated change ($\sim 1‰$) is only a portion of the deglacial and Holocene $\delta^{15}N$ changes reported in fossil-bound $\delta^{15}N$ records (Figure 12b), implying that most of the variation is a direct response of a change in the degree of nitrate consumption in the Southern Ocean.

Figure 11. Time-dependent model experiments in the five-box model start from hypothesized glacial conditions in the Southern Ocean and shift to modern conditions. The perturbation consists of either (a, b) a progressive decrease in the degree of nitrate consumption from 0.95 in both the SAZ and AZ to modern conditions, (c, d) a progressive increase in the overturning ratio from 0.1 to 0.9 (i.e., the degree to which deep water returns to the pycnocline by upwelling in the Southern Ocean as opposed to directly from the deep ocean, Equation 4), or (e, f) both. The black, dark-gray, and light-gray lines in (a, c, e) represent, for each perturbation, the evolution in the overturning ratio and the degree of nitrate consumption in the AZ and SAZ, respectively. For each of these scenarios, the budget-driven nitrate $\delta^{15}N$ remains constant at 6.25‰ (dashed black line in b, d, f), corresponding to the steady state model simulations in which all N_2 fixation and denitrification occur in the pycnocline. The dark blue lines are for the deep ocean, the petrol lines for the AZ surface waters, the olive lines for the combined PFZ-SAZ ventilating area, and the cyan lines for the global pycnocline. The dotted cyan and dark blue lines represent the $\delta^{15}N$ of the pycnocline and the deep ocean, respectively, without N_2 fixation and denitrification (i.e., simulations including only internal nitrate cycling).
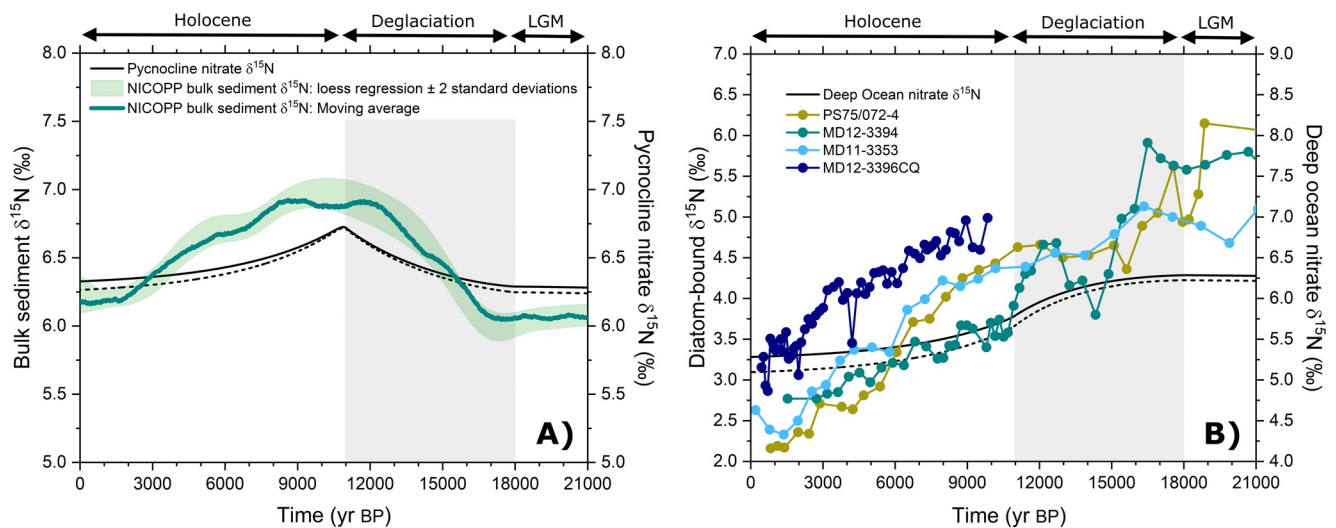
Figure 12. Comparison of time-dependent model experiments (in black with solid and dashed lines for the five-box and nine-box models, respectively) with paleoceanographic N isotope records (in colors) in the mid- and low-latitudes (a) and in the Southern Ocean (b). (a) Comparison between simulated pycnocline nitrate δ^{15}N and a bulk sediment δ^{15}N compilation (NICOPP; Galbraith et al., 2013). For the bulk sediment δ^{15}N compilation, only the records representing the mid- and low-latitudes have been included in the analysis, that is, excluding the records from the Southern Ocean, the Arctic Ocean, and the Mediterranean Sea. The solid green line represents the moving average (2000 years window-length) and the green envelope the two standard deviations from a bootstrap ($n = 1,000$) loess regression analysis (smoothing parameter = 0.33). (b) Comparison between simulated deep ocean nitrate δ^{15}N and diatom-bound δ^{15}N records from the Southern Ocean. Diatom-bound δ^{15}N records are PS75/072-4 in the Pacific Antarctic (olive; Studer et al., 2015), MD12-3394 in the Indian Antarctic (petrol; Ai et al., 2020), MD11-3353 in the Indian Antarctic (cyan; Ai et al., 2020), and MD12-3396CQ in the Indian Polar Frontal Zone (dark blue; Studer et al., 2018). For the time-dependent model experiment, the perturbation includes both a deglacial decrease in the degree of nitrate consumption and a deglacial increase in the overturning ratio (Figures 11e and 11f and Figures S4e and S4f in Supporting Information S1).

4. Conclusions

Our study shows the impact of the Southern Ocean on deep ocean and mean ocean nitrate δ^{15}N that is superimposed on the control by the fixed N budget. Southern Ocean processes drive a nitrate δ^{15}N difference between the pycnocline and the deep ocean. Partial nitrate assimilation in the Southern Ocean raises the δ^{15}N of nitrate in surface waters because of the preferential extraction of ^{14}N for incorporation into new biomass. The upper cell of the meridional overturning circulation transports this high-δ^{15}N nitrate northward and into the pycnocline, while nitrate δ^{15}N in the deep ocean is lowered through the regeneration of complementarily low-δ^{15}N sinking organic matter. This fractionation of N isotopes by the upper cell lowers the nitrate δ^{15}N of the deep ocean relative to the pycnocline. The ocean's fixed N budget fluxes are largely confined to the pycnocline and therefore keep the pycnocline nitrate δ^{15}N close to the budget-driven δ^{15}N value. Consequently, the net effect of Southern Ocean processes is to lower the nitrate δ^{15}N of the deep ocean and thus the mean ocean. The Southern Ocean's impact is a function of both the degree of nitrate consumption in the Southern Ocean surface waters and the relative importance of the Southern Ocean *vs.* the deep ocean in the gross nutrient supply to the global pycnocline (i.e., the "pycnocline recipe") (Figure 9). The findings refine earlier views that (i) the mean ocean nitrate δ^{15}N is solely representative of the sources and sinks of fixed N to the ocean, and that (ii) in the case of a constant oceanic fixed N budget, deep ocean nitrate δ^{15}N must also be constant.

Our findings imply that the nitrate δ^{15}N of the pycnocline as a whole is more representative of the fixed N budget than deep ocean or mean ocean nitrate δ^{15}N. This yields a $\sim$1‰ higher budget-driven nitrate δ^{15}N than previously estimated, and, therefore, a modestly ($\sim$10%–40%) higher ratio of water column to sedimentary denitrification for a given set of isotope effects for these two pathways of oceanic fixed N loss. This, in turn, implies a lower total rate for oceanic denitrification than is calculated without considering the pycnocline-deep ocean nitrate δ^{15}N difference. There are also implications for paleoceanographic N isotope records. First, the ice age increase in the fossil-bound organic matter δ^{15}N in the Southern Ocean may have been amplified by an associated increase in deep ocean nitrate δ^{15}N; this amplification would have been $\sim$1‰, representing $\sim$25% of the full glacial-interglacial δ^{15}N change. Second, roughly $\sim$0.6‰ of the δ^{15}N peak observed during the last deglaciation in many low-latitude N isotope records may reflect the response of the pycnocline to Southern Ocean deglacial changes followed by the relaxation of pycnocline nitrate δ^{15}N to the value required by the ocean's fixed N budget.

Data Availability Statement

The data supporting the findings of this study are available in the PANGAEA database (https://doi.org/10.1594/PANGAEA.936484). The model described in this article is available on ZENODO (https://doi.org/10.5281/zenodo.7574283) and can be used to generate the output reported here.

References

Ai, X. E., Studer, A. S., Sigman, D. M., Martínez-García, A., Fripiat, F., Thöle, L. M., et al. (2020). Southern Ocean upwelling, Earth's obliquity, and glacial-interglacial atmospheric CO_2 change. *Science*, *370*(6522), 1348–1352. https://doi.org/10.1126/science.abd2115

Alkhatib, M., Lehmann, M. F., & de Giorgio, P. A. (2012). The nitrogen isotope effect of benthic remineralization-nitrification-denitrification coupling in an estuarine environment. *Biogeosciences*, *9*(5), 1633–1646. https://doi.org/10.5194/bg-9-1633-2012

Altabet, M. A. (1988). Variations in nitrogen isotopic composition between sinking and suspended particles: Implications for nitrogen cycling and particle transformation in the open ocean. *Deep-Sea Research*, *35*(4), 535–553. https://doi.org/10.1016/0198-0149(88)90130-6

Altabet, M. A. (2007). Constraints on oceanic N balance/imbalance from sedimentary ^{15}N records. *Biogeosciences*, *4*(1), 75–86. https://doi.org/10.5194/bg-4-75-2007

Altabet, M. A., & Francois, R. (1994). Sedimentary nitrogen isotopic ratio as a recorder for surface ocean nitrate utilization. *Global Biogeochemical Cycles*, *8*(1), 103–116. https://doi.org/10.1029/93gb03396

Altieri, K. E., Fawcett, S. E., & Hastings, M. G. (2021). Reactive nitrogen cycling in the atmosphere and ocean. *Annual Review of Earth and Planetary Sciences*, *49*(1), 523–550. https://doi.org/10.1146/annurev-earth-083120-052147

Anderson, R. F., Ali, S., Bradtmiller, L. I., Nielsen, S. H. H., Fleisher, M. Q., Anderson, B. E., & Burckle, L. H. (2009). Wind-driven upwelling in the Southern Ocean and the deglacial rise in atmospheric CO_2. *Science*, *323*(5920), 1443–1448. https://doi.org/10.1126/science.1167441

Barford, C. C., Montoya, J. P., Altabet, M. A., & Mitchell, R. (1999). Steady-state nitrogen isotope effects of N_2 and N_2O production in *Paracoccus denitrifians*. *Applied and Environmental Microbiology*, *65*(3), 989–994. https://doi.org/10.1128/aem.65.3.989-994.1999

Bianchi, D., Dunne, J. P., Sarmiento, J. L., & Galbraith, E. D. (2012). Data-based estimates of suboxia, denitrification, and N_2O production in the ocean and their sensitivities to dissolved O2. *Global Biogeochemical Cycles*, *26*(2), GB2009. https://doi.org/10.1029/2011GB004209

Bohlen, L., Dale, A. W., & Wallmann, K. (2012). Simple transfer functions for calculating benthic fixed nitrogen losses and C:N:P regeneration ratios in global biogeochemical models. *Global Biogeochemical Cycles*, *26*(3), GB3029. https://doi.org/10.1029/2011GB004198

Brandes, J. A., & Devol, A. H. (1997). Isotopic fractionation of oxygen and nitrogen in coastal marine sediments. *Geochimica et Cosmochimica Acta*, *61*(9), 1793–1801. https://doi.org/10.1016/s0016-7037(97)00041-0

Brandes, J. A., & Devol, A. H. (2002). A global marine-fixed nitrogen isotopic budget: Implications for Holocene nitrogen cycling. *Global Biogeochemical Cycles*, *16*(4), 1120–67-14. https://doi.org/10.1029/2001GB001856

Brandes, J. A., Devol, A. H., Yoshinari, T., Jayakumar, D. A., & Naqvi, S. W. A. (1998). Isotopic composition of nitrate in the central Arabian Sea and eastern tropical North Pacific: A tracer for mixing and nitrogen cycles. *Limnology & Oceanography*, *43*(7), 1680–1689. https://doi.org/10.4319/lo.1998.43.7.1680

Brunner, B., Contreras, S., Lehmann, M. F., Kuypers, M. M. M., Rollog, M., Kalvelage, T., et al. (2013). Nitrogen isotope effects induced by anammox bacteria. *Proceedings of the National Academy of Sciences*, *110*(47), 18994–18999. https://doi.org/10.1073/pnas.1310488110

Bryan, F. (1987). Parameter sensitivity of primitive equation ocean general circulation models. *Journal of Physical Oceanography*, *17*(7), 970–985. https://doi.org/10.1175/1520-0485(1987)017<0970:psopeo>2.0.co;2

Buchanan, P. J., Matear, R. J., Chase, Z., Phipps, S. J., & Bindoff, N. L. (2019). Ocean carbon and nitrogen isotopes in CSIRO Mk3L-COAL version 1.0: A tool for paleoceanoghic research. *Geoscientific Model Development*, *12*(4), 1491–1523. https://doi.org/10.5194/gmd-12-1491-2019

Carpenter, E. J., Harvey, H. R., Fry, B., & Capone, D. G. (1997). Biogeochemical tracers of the marine cyanobacterium Trichodesmium. *Deep-Sea Research*, *44*(1), 27–38. https://doi.org/10.1016/s0967-0637(96)00091-x

Casciotti, K. L., Buchwald, C., & McIlvin, M. R. (2013). Implications of nitrate and nitrite isotopic measurements for the mechanism of nitrogen cycling in the Peru oxygen deficient zone. *Deep-Sea Research I*, *80*, 78–93. https://doi.org/10.1016/j.dsr.2013.05.017

Chavaillaz, Y., Codron, F., & Kageyama, M. (2013). Southern westerlies in LGM and future (RCP4.5) climates. *Climate of the Past*, *9*(2), 517–524. https://doi.org/10.5194/cp-9-517-2013

Cline, J. D., & Kaplan, I. R. (1975). Isotopic fractionation of dissolved nitrate during denitrification in the eastern tropical North Pacific Ocean. *Marine Chemistry*, *3*(4), 271–299. https://doi.org/10.1016/0304-4203(75)90009-2

Codispoti, L. A., Brandes, J. A., Christensen, J. P., Devol, A. H., Naqvi, S. W. A., Paerl, H. W., & Yoshinari, T. (2001). The oceanic fixed nitrogen and nitrous oxide budgets: Moving targets as we enter the Anthropocene? *Scientia Marina*, *65*(S2), 85–105. https://doi.org/10.3989/scimar.2001.65s285

Deman, F., Fonseca-Batista, D., Roukaerts, A., García-Ibáñez, M. I., Le Roy, E., Thilakarathne, E. P. D. N., et al. (2021). Nitrate supply routes and impact of internal cycling in the North Atlantic Ocean inferred from nitrate isotopic composition. *Global Biogeochemical Cycles*, *35*(4), e2020GB006887. https://doi.org/10.1029/2020GB006887

Deutsch, C., Gruber, N., Key, R. M., Sarmiento, J. L., & Ganachaud, A. (2001). Denitrification and N_2 fixation in the Pacific ocean. *Global Biogeochemical Cycles*, *15*(2), 483–506. https://doi.org/10.1029/2000gb001291

Deutsch, C., Sarmiento, J. L., Sigman, D. M., Gruber, N., & Dunne, J. P. (2007). Spatial coupling of nitrogen inputs and losses in the ocean. *Nature*, *445*(7124), 163–167. https://doi.org/10.1038/nature05392

Deutsch, C., Sigman, D. M., Thunell, R. C., Meckler, A. N., & Haug, G. H. (2004). Isotopic constraints on glacial/interglacial changes in the oceanic nitrogen budget. *Global Biogeochemical Cycles*, *18*(4), GB4012. https://doi.org/10.1029/2003GB002189

DeVries, T., Deutsch, C., Primeau, F., Chang, B., & Devol, A. (2012). Global rates of water-column denitrification derived from nitrogen gas measurements. *Nature Geoscience*, *5*(8), 547–550. https://doi.org/10.1038/ngeo1515

DeVries, T., Deutsch, C., Rafter, P. A., & Primeau, F. (2013). Marine denitrification rates determined from a global 3-D inverse model. *Biogeosciences*, *10*(4), 2481–2496. https://doi.org/10.5194/bg-10-2481-2013

Dong, S., Sprintall, J., Gille, S. T., & Talley, L. (2008). Southern Ocean mixed-layer depth from Argo float profiles. *Journal of Geophysical Research*, *113*(C6), C06013. https://doi.org/10.1029/2006JC004051

Eugster, O., & Gruber, N. (2012). A probablistic estimate of global marine N-fixation and denitrification. *Global Biogeochemical Cycles*, *26*, GB4013. https://doi.org/10.1029/2012GB004300

Fawcett, S. E., Ward, B. B., Lomas, M. W., & Sigman, D. M. (2015). Vertical decoupling of nitrate assimilation and nitrification in the Sargasso Sea. *Deep-Sea Research I*, *103*, 64–72. https://doi.org/10.1016/j.dsr.2015.05.004

François, R., Altabet, M. A., Yu, E.-F., Sigman, D. M., Bacon, M. P., Frank, M., et al. (1997). Contributions of Southern Ocean surface-water stratification to low atmospheric CO$_2$ concentrations during the last glacial period. *Nature*, *389*(6654), 929–935. https://doi.org/10.1038/40073

Fripiat, F., Declercq, M., Sapart, C. J., Anderson, L. G., Bruechert, V., Deman, F., et al. (2018). Influence of the bordering shelves on nutrient distributions in the Arctic halocline inferred from water column nitrate isotopes. *Limnology & Oceanography*, *63*(5), 2154–2170. https://doi.org/10.1002/lno.10930

Fripiat, F., Marconi, D., Rafter, P., & Sigman, D. M. (2021). Compilation of nitrate δ^{15}N in the ocean. *PANGAEA*. https://doi.org/10.1594/PANGAEA.936484

Fripiat, F., Martínez-García, A., Fawcett, S. E., Kemeny, P. C., Studer, A. S., Smart, S. M., et al. (2019). The isotope effect of nitrate assimilation in the Antarctic Zone: Improved estimates and paleoceanographic implications. *Geochimica et Cosmochimica Acta*, *247*, 261–279. https://doi.org/10.1016/j.gca.2018.12.003

Fripiat, F., Martínez-García, A., Marconi, D., Fawcett, S. E., Kopf, S. H., Lu, V. H., et al. (2021). Nitrogen isotopic constraints on nutrient transport to the upper ocean. *Nature Geoscience*, *14*(11), 855–861. https://doi.org/10.1038/s41561-021-00836-8

Galbraith, E. D., & Kienast, M., & NICOPP working group members. (2013). The acceleration of oceanic denitrification during deglacial warming. *Nature Geoscience*, *6*(7), 579–584. https://doi.org/10.1038/ngeo1832

Garcia, H. E., Locarnini, R. A., Boyer, T. P., Antonov, J. I., Baranova, O. K., Zweng, M. M., et al. (2013). World Ocean Atlas 2013. In S. Levitus, & A. Mishonov Technical (Eds.), *Dissolved Inorganic Nutrients (phosphate, nitrate, silicate)* (Vol. 4, p. 25). NOAA Atlas NESDIS 76. https://doi.org/10.7289/V5J67DWD

Gnanadesikan, A., de Boer, A. M., & Mignone, B. K. (2007). A simple theory of the pycnocline and overturning revisited. In 'Ocean circulation: Mechanisms and impacts'. *Geophysical Monograph Series*, *173*, 19–32.

Granger, J., Prokopenko, M. G., Sigman, D. M., Mordy, C. W., Morse, Z. M., Morales, L. V., et al. (2011). Coupled nitrification-denitrification in sediment of the eastern Bering Sea shelf leads to ^{15}N enrichment of fixed in shelf waters. *Journal of Geophysical Research*, *116*(C11), C11006. https://doi.org/10.1029/2010JC006751

Gruber, N., & Sarmiento, J. L. (1997). Global patterns of marine nitrogen fixation and denitrification. *Global Biogeochemical Cycles*, *11*(2), 235–266. https://doi.org/10.1029/97gb00077

Hendy, I. L., & Pedersen, T. F. (2006). Oxygen minimum zone expansion in the eastern tropical North Pacific during deglaciation. *Geophysical Research Letters*, *33*(20), L20602. https://doi.org/10.1029/2006GL025975

Higginson, M. J., & Altabet, M. A. (2004). Initial test of the silicic acid leakage hypothesis using sedimentary biomarkers. *Geophysical Research Letters*, *31*(18), L18303. https://doi.org/10.1029/2004GL020511

Jaccard, S. L., Hayes, C. T., Martínez-García, A., Hodell, D. A., Anderson, R. F., Sigman, D. M., & Haug, G. H. (2013). Two modes of change in Southern Ocean productivity over the past million years. *Science*, *339*(6126), 1419–1423. https://doi.org/10.1126/science.1227545

Kemeny, P. C., Kast, E. R., Hain, M. P., Fawcett, S. E., Fripiat, F., Studer, A. S., et al. (2018). A seasonal model of nitrogen isotopes in the ice age Antarctic Zone: Support for weakening of the Southern Ocean upper overturning cell. *Paleoceanography and Paleoclimatology*, *33*(12), 1453–1471. https://doi.org/10.1029/2018pa003478

Kienast, M. (2000). Unchanged nitrogen isotopic composition of organic matter in the South China Sea during the last climatic cycle: Global implications. *Paleoceanography*, *15*(2), 244–253. https://doi.org/10.1029/1999pa000407

Knapp, A. N., DiFiore, P. J., Deutsch, C., Sigman, D. M., & Lipschultz, F. (2008). Nitrate isotopic composition between Bermuda and Puerto Rico: Implications for N$_2$ fixation in the Atlantic Ocean. *Global Biogeochemical Cycles*, *22*(3), GB3014. https://doi.org/10.1029/2007GB003107

Knapp, A. N., Sigman, D. M., & Lipschultz, F. (2005). N isotopic composition of dissolved organic nitrogen and nitrate at the Bermuda Atlantic Time-series Study site. *Global Biogeochemical Cycles*, *19*(1), GB1018. https://doi.org/10.1029/2004GB002320

Kohfeld, K. E., Graham, R. M., de Boer, A. M., Sime, L. C., Wolff, E. W., Le Quéré, C., & Bopp, L. (2013). Southern hemisphere westerly wind changes during the last glacial maximum: Paleo-data synthesis. *Quarternary Science Reviews*, *68*, 76–95. https://doi.org/10.1016/j.quascirev.2013.01.017

Kritee, K., Sigman, D. M., Granger, J., Ward, B. B., Jayakumar, A., & Deutsch, C. (2012). Reduced isotope fractionation by denitrification under conditions relevant to the ocean. *Geochimica et Cosmochimica Acta*, *92*, 243–259. https://doi.org/10.1016/j.gca.2012.05.020

Kumar, N., Gwiazda, R., Anderson, R. F., & Froelich, P. N. (1993). ^{231}Pa/^{230}Th ratios in sediments as a proxy for past changes in Southern Ocean productivity. *Nature*, *362*(6415), 46–48. https://doi.org/10.1038/362045a0

Lehmann, M. F., Sigman, D. M., & Berelson, W. M. (2004). Coupling the ^{15}N/^{14}N and ^{18}O/^{16}O of nitrate as a constraint on benthic nitrogen cycling. *Marine Chemistry*, *88*(1–2), 1–20. https://doi.org/10.1016/j.marchem.2004.02.001

Lehmann, M. F., Sigman, D. M., McCorkle, D. C., Granger, J., Hoffmann, S., Cane, G., & Brunelle, B. G. (2007). The distribution of nitrate ^{15}N/^{14}N in marine sediments and the impact of benthic nitrogen loss on the isotopic composition of oceanic nitrate. *Geochimica et Cosmochimica Acta*, *71*(22), 5384–5404. https://doi.org/10.1016/j.gca.2007.07.025

Liu, K.-K., & Kaplan, I. R. (1989). The eastern tropical Pacific as a source of ^{15}N-enriched nitrate in seawater off southern California. *Limnology & Oceanography*, *34*(5), 820–830. https://doi.org/10.4319/lo.1989.34.5.0820

Lumpkin, R., & Speer, K. (2007). Global Ocean meridional overturning. *Journal of Physical Oceanography*, *37*(10), 2550–2562. https://doi.org/10.1175/jpo3130.1

Luo, Y.-W., Doney, S. C., Anderson, L. A., Benavides, M., Berman-Frank, I., Bode, A., et al. (2012). Database of diazotrophs in global ocean: Abundance, biomass and nitrogen fixation rates. *Earth System Science Data*, *4*(1), 47–73. https://doi.org/10.5194/essd-4-47-2012

Marconi, D., Kopf, S., Rafter, P. A., & Sigman, D. M. (2017). Aerobic respiration along isopycnal leads to overestimation of the isotope effect of denitrification in the ocean water column. *Geochimica et Cosmochimica Acta*, *197*, 417–432. https://doi.org/10.1016/j.gca.2016.10.012

Marconi, D., Sigman, D. M., Casciotti, K. L., Campbell, E. C., Weigand, M. A., Fawcett, S. E., et al. (2017). Tropical dominance of N$_2$ fixation in the North Atlantic Ocean: Tropical lead of Atlantic N$_2$ fixation. *Global Biogeochemical Cycles*, *31*(10), 1608–1623. https://doi.org/10.1002/2016gb005613

Marconi, D., Weigand, M. A., Rafter, P. A., McIlvin, M. R., Forbes, M., Casciotti, K. L., & Sigman, D. M. (2015). Nitrate isotope distributions on the US GEOTRACES North Atlantic cross-basin section: Signals of polar nitrate sources and low latitude nitrogen cycling. *Marine Chemistry*, *177*, 143–156. https://doi.org/10.1016/j.marchem.2015.06.007

Marconi, D., Weigand, M. A., & Sigman, D. M. (2019). Nitrate isotopic gradient in the North Atlantic Ocean and the nitrogen isotopic composition of sinking organic matter. *Deep-Sea Research I*, *145*, 109–124. https://doi.org/10.1016/j.dsr.2019.01.010

Marshall, J., & Speer, K. (2012). Closure of the meridional overturning circulation through Southern Ocean upwelling. *Nature Geoscience*, *5*(3), 171–180. https://doi.org/10.1038/NGEO1391

Martin, T. S., & Casciotti, K. L. (2017). Paired N and O isotopic analysis of nitrate and nitrite in the Arabian Sea oxygen deficient zone. *Deep-Sea Research I*, *121*, 121–131. https://doi.org/10.1016/j.dsr.2017.01.002

Martin, T. S., Primeau, F., & Casciotti, K. L. (2019). Modeling oceanic nitrate and nitrite concentrations and isotopes using a 3-D inverse N cycle model. *Biogeosciences*, *16*(2), 347–367. https://doi.org/10.5194/bg-16-347-2019

Martínez-García, A., Sigman, D. M., Ren, H., Anderson, R. F., Straub, M., Hodell, D. A., et al. (2014). Iron fertilization of the Subantarctic Ocean during the last ice age. *Science*, *343*(6177), 1347–1350. https://doi.org/10.1126/science.1246848

McRose, D. L., Lee, A., Kopf, S. H., Baars, O., Kraepiel, A. M. L., Sigman, D. M., et al. (2019). Effect of iron limitation on the isotopic composition of cellular and released fixed nitrogen in *Azotobacter vinelandii*. *Geochimica et Cosmochimica Acta*, *244*, 12–23. https://doi.org/10.1016/j.gca.2018.09.023

Middelburg, J. J., Soetart, K., Herman, P. M. J., & Heip, C. H. R. (1996). Denitrification in marine sediments: A model study. *Global Biogeochemical Cycles*, *10*(4), 661–673. https://doi.org/10.1029/96gb02562

Minagawa, M., & Wada, E. (1986). Nitrogen isotope ratios of red tide organisms in the East China Sea: A characterization of biological nitrogen fixation. *Marine Chemistry*, *19*(3), 245–259. https://doi.org/10.1016/0304-4203(86)90026-5

Morrison, A. K., & Hogg, A. M. (2012). On the relationship between Southern Ocean overturning and ACC transport. *Journal of Physical Oceanography*, *42*, 140–148.

Mortlock, R. A., Charles, C. D., Froelich, P. N., Zibello, M. A., Saltzman, J., Hays, J. D., & Burckle, L. H. (1991). Evidence for lower productivity in the Antarctic Ocean during the last glaciation. *Nature*, *351*(6323), 220–223. https://doi.org/10.1038/351220a0

Munk, W., & Wunsch, C. (1998). Abyssal recipes II: Energetics of tidal and wind mixing. *Deep-Sea Research* I, *45*(12), 1977–2010. https://doi.org/10.1016/s0967-0637(98)00070-3

Pichevin, L. E., Ganeshram, R. S., Francavilla, S., Arellano-Torres, E., Pedersen, T. F., & Beaufort, L. (2010). Interhemispheric leakage of isotopically heavy nitrate in the eastern tropical Pacific during the last glacial period. *Paleoceanography*, *25*(1), PA1204. https://doi.org/10.1029/2009PA001754

Rafter, P. A., DiFiore, P. J., & Sigman, D. M. (2013). Coupled nitrate nitrogen and oxygen isotopes and organic matter remineralization in the Southern and Pacific Oceans. *Journal of Geophysical Research*, *118*(10), 1–14. https://doi.org/10.1002/jgrc.20316

Robinson, R. S., & Sigman, D. M. (2008). Nitrogen isotopic evidence for a poleward decrease in surface nitrate within the ice age Antarctic. *Quaternary Science Reviews*, *27*(9–10), 1076–1090. https://doi.org/10.1016/j.quascirev.2008.02.005

Ryabenko, E., Kock, A., Bange, H. W., Altabet, M. A., & Wallace, D. W. R. (2012). Contrasting biogeochemistry of nitrogen in the Atlantic and Pacific oxygen minimum zones. *Biogeosciences*, *9*(1), 203–215. https://doi.org/10.5194/bg-9-203-2012

Sarmiento, J. L., Gruber, N., Brzezinski, M. A., & Dunne, J. P. (2004). High-latitude controls of thermocline nutrients and low latitude biological productivity. *Nature*, *427*(6969), 56–60. https://doi.org/10.1038/nature02127

Sigman, D. M., Altabet, M. A., McCorkle, D. C., Francois, R., & Fischer, G. (1999). The δ^{15}N of nitrate in the Southern Ocean: Consumption of nitrate in surface waters. *Global Biogeochemical Cycles*, *13*(4), 1149–1166. https://doi.org/10.1029/1999gb900038

Sigman, D. M., Altabet, M. A., McCorkle, D. C., Francois, R., & Fischer, G. (2000). The δ^{15}N of nitrate in the Southern Ocean: Nitrogen cycling and circulation in the ocean interior. *Journal of Geophysical Research*, *105*(C8), 19599–19614. https://doi.org/10.1029/2000jc000265

Sigman, D. M., DiFiore, P. J., Hain, M. P., Deutsch, C., Wang, Y., Karl, D. M., et al. (2009). The dual isotopes of deep nitrate as a constraint on the cycle and budget of oceanic fixed nitrogen. *Deep-Sea Research I*, *56*(9), 1419–1439. https://doi.org/10.1016/j.dsr.2009.04.007

Sigman, D. M., Fripiat, F., Studer, A. S., Kemeny, P. C., Martínez-García, A., Hain, M. P., et al. (2021). The Southern Ocean during the ice ages: A review of the Antarctic surface isolation hypothesis, with comparison to the North Pacific. *Quaternary Science Reviews*, *254*, 106732. https://doi.org/10.1016/j.quascirev.2020.106732

Sigman, D. M., Granger, J., Di Fiore, P. J., Lehmann, M. F., Ho, R., Cane, G., & van Geen, A. (2005). Coupled nitrogen and oxygen isotope measurements of nitrate along the eastern North Pacific margin. *Global Biogeochemical Cycles*, *19*(4), GB4022. https://doi.org/10.1029/2005GB002458

Sime, L. C., Kohfeld, K. E., Le Quéré, C., Wolff, E. W., de Boer, A. M., Graham, R. M., & Bopp, L. (2013). Southern hemisphere westerly wind changes during the last glacial maximum: Model-data comparison. *Quaternary Science Reviews*, *64*, 104–120. https://doi.org/10.1016/j.quascirev.2012.12.008

Somes, C. J., Oschlies, A., & Schmittner, A. (2013). Isotopic constraints on the pre-industrial oceanic nitrogen budget. *Biogeosciences*, *10*(9), 5889–5910. https://doi.org/10.5194/bg-10-5889-2013

Studer, A. S., Mekik, F., Ren, H., Hain, M. P., Oleynik, S., Martínez-García, A., et al. (2021). Ice age-Holocene similarity of foraminifera-bound nitrogen isotope ratios in the Eastern Equatorial Pacific. *Paleocanography Paleoclimatology*, *36*(5). https://doi.org/10.1029/2020PA004063

Studer, A. S., Sigman, D. M., Martínez-García, A., Thöle, L. M., Michel, E., Jaccard, S. L., et al. (2018). Increased nutrient supply to the Southern Ocean during the Holocene and its implications for the pre-industrial atmospheric CO_2 rise. *Nature Geoscience*, *11*(10), 756–761. https://doi.org/10.1038/s41561-018-0191-8

Studer, A. S., Sigman, D. M., Martínez-García, A. M., Benz, V., Winckler, G., Kuhn, G., et al. (2015). Antarctic Zone nutrient conditions during the last two glacial cycles. *Paleoceanography*, *30*(7), 845–862. https://doi.org/10.1002/2014pa002745

Talley, L. D. (2013). Closure of the global overturning circulation through the Indian, Pacific, and Southern Oceans: Schematics and transports. *Oceanography*, *26*(1), 80–97. https://doi.org/10.5670/oceanog.2013.07

Thunnel, R. C., & Kepple, A. B. (2004). Glacial-Holocene delta N-15 record from the Gulf of Tehuantepec, Mexico: Implications for denitrification in the eastern tropical Pacific and changes in atmospheric N_2O. *Global Biogeochemical Cycles*, *18*(1), GB1001. https://doi.org/10.1029/2002GB002028

Toggweiler, J. R., Russell, J. L., & Carson, S. R. (2006). Midlatitude westerlies, atmospheric CO_2, and climate change during ice ages. *Paleoceanography*, *21*, PA2005. https://doi.org/10.1029/2005PA001154

Voss, M., Dippner, J. W., & Montoya, J. P. (2001). Nitrogen isotope patterns in the oxygen-deficient waters of the Eastern Tropical North Pacific Ocean. *Deep-Sea Research I*, *48*(8), 1905–1921. https://doi.org/10.1016/s0967-0637(00)00110-2

Wang, W.-L., Moore, J. K., Martiny, A. C., & Primeau, F. W. (2019). Convergent estimates of marine nitrogen fixation. *Nature*, *566*(7743), 205–210. https://doi.org/10.1038/s41586-019-0911-2

Wang, X. T., Sigman, D. M., Propopenko, M. G., Adkins, J. F., Robinson, L. F., Hines, S. K., et al. (2017). Deep-sea coral evidence for lower Southern Ocean surface nitrate concentration during the last ice age. *Proceedings of the National Academy of Sciences*, *114*(13), 3352–3357. https://doi.org/10.1073/pnas.1615718114

Yang, S., & Gruber, N. (2016). The anthropogenic perturbation of the marine nitrogen cycle by atmospheric deposition: Nitrogen cycle feedbacks and the ^{15}N Haber-Bosh effect. *Global Biogeochemical Cycles*, *30*(10), 1418–1440. https://doi.org/10.1002/2016gb005421